Alpha cell inflammation during human pancreas aging and type 2 diabetes and its reversal by calorie restriction in mice.

Michael Schleh[1], Jean-Philippe Cartailler[2], Shristi Shrestha[2], Amanda Cambraia[1], Aliyah Habashy[1], Cara Ellis[3], Melanie Cutler[1], Gabriel Ferguson[1], Alvin Powers[4], Rafael Arrojo e Drigo[1,4,5,6*]

[1] Department of Molecular Physiology and Biophysics, Vanderbilt University School of Medicine, Nashville, TN
[2] Creative Data Solutions, Center for Stem Cell Biology, Vanderbilt University School of Medicine, Nashville, TN
[3] Alberta Diabetes Institute and Department of Pharmacology, University of Alberta, Edmonton, Canada
[4] Vanderbilt Diabetes Research and Training Center, Vanderbilt University Medical Center, Nashville, TN
[5] Center for Cell Systems Biology, Vanderbilt University School of Medicine, Nashville, TN
[6] Mass Spectrometry Research Center, Vanderbilt University School of Medicine, Nashville, TN
*Corresponding author

Keywords: aging, alpha cells, antigen presentation, calorie restriction, T cells

Address of Correspondence:
Rafael Arrojo e Drigo
718 Light Hall
2215 Garland Ave
Nashville, Tennessee 37232
r.drigo@vanderbilt.edu

Running Title: Alpha cell inflammation and calorie restriction in aging

Abstract (145/150)

Aging increases risk for type 2 diabetes (T2D), partly through loss of beta cell identity and function driven by metabolic stress and islet inflammation. While calorie restriction (CR) promotes beta cell longevity in young animals, its impact on cellular aging and inflammatory burden in older individuals is unclear. Using SCENIC regulon and multiomic analyses, we find that aging human alpha cells adopt a coordinated inflammatory phenotype marked by IFN-γ signaling to increase major histocompatibility complex (MHC) class I presentation, and $CD8^+$ T cell recruitment and activation towards islets. In T2D, $CD8^+$ T cells further progress towards an effector memory state. CR reduces alpha cell MHC-I expression while subsequently suppressing $CD8^+$ effector status and accompanied by reduced islet inflammation and immune cell infiltration in mice. Together, these findings highlight an alpha cell–immune signaling axis in aging and T2D that may underlie fibrosis and disease pathophysiology.

Introduction

Aging is a major risk factor for type 2 diabetes (T2D), with prevalence reaching 28.8% among adults aged ≥65 years in the United States (*1*). Age-related deterioration in glycemic control has largely been attributed to progressive insulin resistance, impaired beta cell insulin secretion, and altered hepatic insulin clearance (*2-4*). However, aging is also characterized by tissue loss of homeostatic resilience and increased immune heterogeneity, that may shape metabolic health decline (*5*). A central feature of adaptive immune aging is thymic involution, which reduces naïve T cell output and shifts the T cell compartment towards peripheral expansion and memory biased populations (*6-8*). Whether such age-associated immune remodeling arises primarily through intrinsic programs or occurs secondary to extrinsic cues in the microenvironment and whether these aspects are present during diabetes, remains largely unknown.

Pancreatic islets are composed primarily of long-lived endocrine alpha- and beta cells, which maintain glucose homeostasis through coordinated secretion of glucagon and insulin (*9-12*). During aging, beta cells exhibit structural and functional decline, including loss of cellular identity, DNA damage accumulation, endoplasmic reticulum (ER) stress, impaired autophagy, increased transcriptional noise, amyloid deposition, senescence, and accumulate islet fibrosis (*2, 13-16*). In contrast, far less is known how aging affects alpha cell biology despite well-known disruptions in alpha cell glucagon secretion during aging and along the natural history of T2D (*2, 17-20*) that are accompanied by exaggerated amino acid-induced glucagon release (*21, 22*). Moreover, it remains unknown whether aging promotes intrinsic inflammatory programs within specific endocrine cell types, or whether islet inflammation is driven predominantly by extrinsic immune cues. Defining the cellular origins of age-associated islet inflammation is essential to understanding the intersection of immune and metabolic aging and how these aspects may contribute to diabetes pathogenesis.

Calorie restriction (CR) is a well-established dietary intervention that extends lifespan and health span across species by delaying several hallmarks of cellular dysfunction during aging (*23-26*). Moderate energy restriction (10–40%) improves metabolic homeostasis in both young and aged animals, in part through modulation of nutrient-sensing pathways including insulin-IGF1, mTORC1, and AMPK (*27, 28*). CR also reduces oxidative stress and inflammatory tone while enhancing autophagy and proteostasis (*29-31*), and it can promote anti-inflammatory responses in lean adult humans (*32*). In young adult mice, CR and CR-mimicking interventions improve beta cell function and longevity, and which are thought to be explained by enhanced peripheral insulin sensitivity (*33-36*). However, whether CR can reverse established age-associated islet inflammation, particularly within specific endocrine cell populations, remains unresolved.

Here, we integrated multimodal and multiomic analyses of publicly available human islet datasets – including bulk proteomics, singe-cell RNA sequencing (scRNA-seq) and epigenome profiling, and spatial proteomics – and performed a large-scale meta-analysis to define the molecular signatures of alpha cells during aging in non-diabetic (ND) donors and to determine their relevance to T2D. At the islet proteome level, human islets exhibited hallmarks of ER stress, senescence, and inflammatory activation linked to innate and adaptive signaling compartments. Single cell transcriptomics revealed these inflammatory signatures were significantly enriched in alpha cells and these resulted from IFN-γ-induced pro-inflammatory signaling via activation of pro-inflammatory transcription factors (TFs) STAT1, IRF1, and NFKB1. Notably, this pro-inflammatory alpha cell state is linked to increased amino-acid induced glucagon release in vitro, which may explain previous observations of hyperglucagonemia in ND humans in vivo (*2*). Moreover, spatial proteomics confirmed this pro-inflammatory signaling in alpha cells correlates with increased abundance of major histocompatibility complex class I (MHC-I; HLA-ABC) in alpha cells from aged donors, and which associated with enrichment of $CD8^+$ T cells within the

islet microenvironment and closer to alpha cells, specifically. In T2D, these islet CD8+ T cells suffer a shift towards central memory and terminally differentiated $CD8^+$ phenotypes. Similarly, we show in old mice that this alpha cell-immune association is active, and it can be successfully reversed by short term CR, which is sufficient to reduce alpha cell inflammation and attenuate $CD8^+$ T cell effector islet accumulation.

Together, our study identifies alpha cell inflammation as a previously unrecognized hallmark of human pancreas aging that is molecularly and functionally distinct from aging beta cells. These findings establish a link between alpha cell pro-inflammatory programs and adaptive immune activation during aging and demonstrate that CR can reverse age-associated islet immune dysfunction by modulating alpha cells and to preserve systemic metabolic homeostasis.

Results

Aging ND islets exhibit elevated immune activity and unfolded protein response signaling. Islet inflammation and fibrosis are hallmarks of human pancreas aging and diabetes, contributing to beta cell dysfunction (*37-39*). To define proteomic signatures of aging, we leveraged the HumanIslets consortium dataset comparing young (28±4 years, n=26) and old (71±3 years, n=19) ND donors (**Figure 1A, Supplementary Table S1A-S1B**) (*40, 41*). Aging was associated with 86 increased and 17 decreased proteins (**Supplementary Table S2**). Pathway analysis (Reactome) revealed enrichment of innate immune signaling, alongside elevated amino acid metabolism, mTORC1 activity, and ER stress pathways in old adults (**Figure 1B, Supplementary Table S3**). Consistent with these changes, aged islets exhibited increased markers of beta cell immaturity (RBP4 (*42*); **Figure 1C**), senescence (CDKN1A/p21 (*43*), **Figure 1D**), ER stress signaling (ATF6, CHOP, PERK; **Figure 1E**), and mTORC1 activation (LAMP2, LAMTOR, RAGA, RAGC; **Figure 1F**). A robust immune signature was also evident by upregulation of antigen presentation (HLA-A), T-cell receptor (TCR) signaling and memory proteins (CD28, CD44), and immune-regulatory signaling (TGF-β1, TOM1, CD63; **Figure 1G**). Together, these findings reinforce aging human islets exhibit coordinated ER stress and metabolic remodeling alongside heightened inflammatory and immune engagement within the islet microenvironment.

Single cell transcriptomics reveal inflammatory signaling in aging human alpha cells. Over the past decade, single-cell approaches have defined how islet gene regulation changes during development, aging, and diabetes (*42, 44-53*). We previously showed that aging ND beta cells exhibit chronic ER stress and loss of identity and insulin secretion (*44*), and further supported by our proteomic findings (**Figure 1**). To identify specific cell types contributing to the inflammatory signatures observed in aging islets, we analyzed scRNA-seq data from a uniformly re-processed dataset created by PanKbase based on previously published studies (*54, 55*). After quality control and cohort selection, the final dataset annotated 131,610 islet cells from 32 donors (56,851 alpha cells), stratified into young (20-40 years) and old (≥50 years) groups (**Supplementary Figure S1A-C, Supplementary Table S4A-S4B).**

Among ND islet endocrine cell types, alpha cells exhibited the highest expression of MHC-I genes (HLA-ABC), followed by immune, ductal, and endothelial cells (**Supplementary Figure S1D**). Pseudobulk differential expression and gene set enrichment analysis (GSEA) across alpha, beta, acinar, and MUC5B ductal cells identified age-dependent transcriptomic changes for major islet and pancreas cell types (**Figure 2B, Supplementary Figure S1E, Supplementary Table S5**). This approach revealed activation of type II interferon (IFN-γ) signaling in aging alpha, beta, and acinar cells (**Figure 2C and Supplementary Figure S1F**). To deconvolve the impact of IFN-γ within the human islet cytoarchitecture, we performed weighted analysis of IFN-γ responsive genes enriched in old alpha cells and beta cells and discovered that canonical IFN-γ signaling is strongly enriched in old alpha cells (**Figure 2D, Supplementary Figure S2A-S2B**). Old alpha cells displayed canonical IFNγ signatures, including activation of JAK-

STAT (*STAT1*, *SOCS1*, *SOCS3*, *IRF7/9*, *IL7*, and *IL15*) and antigen processing pathways (*TAP1, B2M*), whereas old beta cells display TNF-signaling pathway signatures (**Figure 2D-E, Supplementary Figure S2C-S2D**). As expected, this analysis also found activation of ER stress and DNA damage, and impaired oxidative phosphorylation in old beta cells (*44*). None of these are found in old alpha cells (**Supplementary Figure S1F, S2A-S2B, Supplementary Table 6**). Old alpha cells also increased expression of senescence-associated genes (*IGF1R, CDKN2A, CDKN1A/B*) and of alpha cell identity markers (*ALDH1A1, TM4SF4, LOXL4)*, while displaying reduced expression of ER stress-related genes (HERPUD1, ATF4, JUND). This data hints that aging alpha cells may develop senescence next to old beta cells however they do not suffer from significant impairments to identity or activation of ER stress (**Supplementary Figure S1G**) (*56, 57*). Importantly, unlike old acinar cells, old alpha cells and beta cells did not display significant activation of pro-apoptosis pathways (**Supplementary Figure S1H**), thus suggesting that this pro-inflammatory environment does not lead to loss of alpha or beta cells.

Aging alpha cells also had increased expression of genes across several metabolic processes including glucose metabolism and oxidative phosphorylation, fatty acid metabolism, and amino acid catabolism (**Figure 2F-G and Supplementary Figure S1I**). To determine if these transcriptional changes correlate with alterations in alpha cell glucagon secretion, we analyzed HPAP human islet perifusion data from young and old adult donors from two different human islet analysis centers (UPenn and Vanderbilt), which used complementary stimulation protocols to test for the effect of several insulin and glucagon secretagogues. This revealed that alpha cells from older donors have increased glucagon secretion in response to stimulation with a mixed amino acid (AA) cocktail and to de-polarization with KCL (**Figure 2H-K**). No changes were observed when alpha cells were stimulated with low glucose, high glucose, and epinephrine (**Supplementary Figure S3**).

Together, these results indicate that aging human alpha cells acquire senescence-associated features, display heightened AA-dependent glucagon secretion, and an active IFN-γ signaling coupled with MHC-I antigen-presentation programs.

Re-organization of gene regulatory networks activates inflammatory gene expression in aging alpha cells. We have previously applied the transcription factor (TF) inference algorithm pySCENIC (*58*) to show that aging beta cell stress arises from reconfigured gene regulatory networks (GRNs) and activation of stress TFs (*44*). Here, we used pySCENIC and graph network analysis to characterize GRNs in aging alpha cells and identify the TFs linked to activation of the observed inflammatory response. This approach identified TFs enriched in both age groups (**Figure 3A**), including canonical alpha cell TFs (NKX6-1,FOXA2), and inflammation-associated TFs that were significantly enriched in old alpha cells (IRFs, NFKB1, and STAT1) (**Figure 3A, Supplementary Figure S4**).

We reconstructed enriched GRNs of young and old alpha cells and observed a stronger inferred activity of pro-inflammatory TFs (IRF1, NFKB1, and STAT1 signaling) and reduced activity of MAFB during aging (**Figure 3B**). This data suggests that although inflammation-associated TFs are found in both age groups, these TFs play a relatively small role in the overall transcriptome landscape in younger alpha cells. To test this hypothesis, we performed analysis of TF-associated regulons to reveal that inflammatory TFs do not target the same set of genes in young versus old alpha cells, suggesting a significant re-wiring of alpha cell GRNs during aging. This is characterized by a low Jaccard similarity index between conserved TFs in both age groups, and this includes loss of TF-regulon similarity for alpha cell identity TFs (ARX, HNF1A, HNF4A) as well as inflammation-associated TFs (STAT1, IRF2/7/8/9). In fact, these TFs are redirected towards new targets that include several genes identified as part of the pro-inflammatory signaling phenotype of old alpha cells (**Figure 3C**, **Supplementary Table S7**). Moreover, several of these downstream gene targets were pro-inflammatory TFs themselves, which

203 created a pro-inflammatory TF network in old alpha cells centered around NFKB1 and IRF1
204 (**Figure 3D**). In contrast, old alpha cells lose the link between NKX6.1, MAFB, and ISL1 that is
205 only observed in young cells (**Figure 3D**).

206 To further validate our SCENIC results, we integrated our analysis with publicly available
207 chromatin accessibility data from HPAP (snATAC-seq). Here, we performed differential analysis
208 of peak accessibility using ChromVAR (*59*) to identify TF motifs enriched in chromatin regions
209 significantly upregulated in old alpha cells. Next, we crossed referenced this list with our old al-
210 pha cell SCENIC data to identify n=269 shared TFs, including canonical alpha cell TFs (FOXA2,
211 HNF1A/B) and several inflammatory TFs (IRFs, KLF6, NFKB1/RELs, STAT1) (**Figure 3E**).

212 These data indicate that aging promotes re-wiring of alpha cell GRNs to activate inter-
213 feron-stimulated NFKB1, IRF1, and STAT1 gene expression programs and this likely explains
214 the origins of pro-inflammatory activation in aging alpha cells.

215 **Spatial analysis of aging human pancreases identifies alpha cell-T-cell interactions *in***
216 ***situ*.** Aging ND human pancreases exhibit multiple features of chronic low-grade inflammation,
217 including increased fibrosis, higher incidence of acinar-to-ductal metaplasia (ADM), angiopathy,
218 and pancreatic adiposity (*38, 39*). To validate our proteomic and transcriptomics meta-analysis
219 findings *in situ*, we analyzed high-dimensional imaging mass cytometry (IMC) and CO-Detection
220 by indexing (CODEX) datasets from HPAP (*60, 61*). Human ND pancreas samples were strati-
221 fied into younger adult (22-40 years) and older adults (47-58 years) groups (**Supplementary**
222 **Figure S5B and S6B; Supplementary Tables S8 and S9).** Individual cells from each donor im-
223 age were segmented using standard QuPath- and Seurat-based workflows for cell identification
224 and spatial annotation, cell marker quantification, and unsupervised clustering (**Supplementary**
225 **Figure S5A and S6A)**. This allowed us to identify and map the spatial landscape of major pan-
226 creatic cells including alpha cells (GCG^+), beta cells ($C\text{-}peptide^+$), delta cells (SST^+), pancreatic
227 polypeptide cells (PP^+), endothelial cells ($CD31^+$), Epithelial/Acinar cells ($CK19^+/CA2^+$), M1-like
228 macrophages ($CD45^+CD68^+CD163^-$), M2-like macrophages ($CD45^+CD68^+CD163^+$), and $CD4^+$
229 and $CD8^+$ T cell subpopulations ($CD45^+CD3^+CD4^+$ and $CD45^+CD3^+CD8^+$, respectively) (**Figure**
230 **4A and 4C, Supplementary Figures S5C-G and S6C-G, Supplementary Tables S10-S11**).

231 This framework enabled spatial mapping of all major pancreatic and immune cell types
232 in both IMC (**Figure 4A-B**) and CODEX (**Figure 4C-D, Supplementary Figure S7A**) platforms
233 to quantify immune and endocrine cell composition and their molecular phenotypes. Using this
234 approach, we found no differences in endocrine islet cell composition (**Supplementary Figure**
235 **S7B**) and expected age-associated decreases in beta cell identity markers PDX-1, NKX6-1, and
236 PAX6 (**Supplementary Figure S7C**) (*44*). This data confirms loss of beta cell identity during ag-
237 ing without the activation of cell death (*39, 44*). Importantly, we found that ND aging pancreases
238 have significant expansion of $CD45^+CD3^+$ T cells predominantly driven by accumulation of $CD8^+$
239 T-cells that can be found inside the islet (**Figure 4B, 4D-E, and Supplementary Figure S7D**
240 **and S8A**). No age-associated differences were detected for $CD4^+$ T cells or in total macrophage
241 density (**Figure 4F-G**).

242 To further investigate the organization of endocrine-immune interactions underlying
243 $CD8^+$ T-cell expansion, we utilized spatial coordinates to identify nearest-neighbor cell endocrine
244 beta and alpha cells within a 50μm radius of CD8 T cells, as established previously by other
245 groups (*62-64*). This revealed that older pancreases have a higher fraction of $CD8^+$ T cells in the
246 vicinity or in direct contact with alpha cells (**Figure 4E and 4H, Supplementary Figure S8A**),
247 which was not observed for beta cells (**Figure 4I**).

248 During an inflammatory event, $CD8^+$ T cells engage neighboring cells by interaction be-
249 tween the T cell receptor (TCR) and major histocompatibility complex class 1 (MHC-1) mole-
250 cules on the interacting cell. Accordingly, the increased spatial proximity between alpha cells

and CD8$^+$ T cells correlated with a significant increase in the expression of MHC-I complex HLA-ABC molecules in alpha cells (**Figure 4J**). In fact, older alpha cells express ~5x more HLA-ABC than neighboring beta cells, and both cell types express near background levels of MHC-II HLA-DR molecules (**Figure 4L**). Because alpha cell mass was unchanged with aging, this suggests that despite significant interactions between alpha cells and CD8$^+$ T cells, aging is not associated with alpha cell loss (as indicated by the single-cell transcriptomics data (**Supplementary Figure S1H**).

Together, these findings demonstrate that human islet and pancreatic aging landscapes are defined by increased pro-inflammatory signaling from alpha cells that correlates with elevated CD8$^+$ T-cell density *in situ*. Given that MHC molecules present antigenic peptides to T cells via TCR engagement, these results suggest that alpha cell-intrinsic inflammatory pathways may orchestrate immune activation and islet inflammation during aging.

T2D expands pancreatic CD8$^+$ T cells that shift towards terminal effector-memory phenotypes. To determine how these pancreas and immune aging signatures overlap with T2D pathogenesis, we analyzed CODEX data from T2D donors profiled through HPAP (**Supplementary Table S12**). Cohorts were matched for age and BMI; however, T2D donors displayed expected impairments in glycemia, evidenced by higher HbA1c and reduced C-peptide (**Figure 5A**). Integration of 942,724 single-cell profiles identified and characterized endocrine (99,744 cells) and immune (195,140 cells) compartments (**Figure 5B**). Our endocrine cell clustering approach identified no changes to major islet cell populations and highlighted two distinct beta cell populations: a CPEP$^+$CHGA$^+$ population and a CPEP$^+$CHGA$^+$COL4A1$^+$COL6$^+$ population that was enriched in T2D (**Figure 5C**). These cells exhibited higher interaction with fibrotic extra-cellular matrix (ECM) and thus were detected as being “fibrotic” by our expansion-based cell segmentation algorithms that captured ECM signals from neighboring regions (**Supplementary Figure S8A**). Importantly, T2D beta cells were marked by lower CPEP, CHGA, NKX6-1 expression (**Figure 5D**), while alpha cells had attenuated SOX9 (**Figure 5E**), consistent with compromised endocrine cell identity during T2D (*65*). Within immune compartments, we observed no changes in macrophages densities (**Figure 5F**), and a significant ~2-fold increase in pancreas CD8$^+$ T-cell density (**Figure 5G**). Together, these findings demonstrate that T2D amplifies CD8$^+$ T-cell density to mirror patterns observed during aging in ND pancreases.

To resolve whether the increased adaptive immune phenotype observed in both aging and T2D pancreases was localized within islets, we analyzed HPAP cytometry by time-of-flight (CyTOF) data from isolated islets of young (26±8 years, n=13), old (54±5 years, n=14), and T2D (50±8 years, n=13) human donors (**Figure 5H, Supplementary Table S13-14**). Both aging and T2D presented greater CD45$^+$ live immune cell abundance compared with young adults, corresponding with higher frequencies of islet CD8$^+$ T cells within the CD45$^+$ immune compartment (**Figure 5I-J, Supplementary Figure S9**). CD8$^+$ T cells differentiate along a spectrum from naïve (CD8$_{naïve}$) to CD8$_{CM}$ and CD8$_{TEM}$ states in response to TCR activation by antigen and cytokine stimulation. In T2D islets, we observed a reduction in CD45RA$^+$CD27$^+$ CD8$_{naïve}$ T cells compared to young adults, whereas aging increased CD45RA$^-$CD27$^+$ CD8$_{CM}$ T cells (**Figure 5K-L**). T2D islets further shifted CD8$^+$ T-cell populations towards a higher CD45RA$^+$CD27$^-$ CD8$_{TEM}$ phenotype, resulting in elevated effector-to-central memory ratio that was not observed in aging ND samples (**Figure 5L-M**).

Together, these data show that T2D intensifies pancreas and islet CD8$^+$ T-cell infiltration patterns found during aging to drive their progression towards terminal effector-memory states.

Calorie restriction improves glucose tolerance and dampens alpha cell inflammation in mice. CR is a dietary intervention approach that can normalize glycemia during prediabetes and T2D, likely by delaying the onset of workload stress and aging hallmarks in beta cells (*32, 66-*

69). We therefore tested whether CR could reverse aging signatures in alpha and beta cells *in vivo*. To achieve this, 72-week-old C57BL/6J male mice were subjected to a 2-month, 20% CR feeding regimen, while age-matched controls remained on ad-libitum (AL) diet (**Figure 6A**). As expected, CR mice consumed 80% of total kcal intake compared to AL-fed controls (**Supplementary Figure S10A-B**). This intervention induced a steady decline in body weight over 2 months, resulting in ~12% weight loss (**Figure 6B, Supplementary Figure S10C-D**) predominantly due to a loss in fat mass (**Supplementary Figure S10E-F**). Of note, CR mice also experienced reductions in liver and epididymal white adipose tissue (eWAT) mass due to reduced lipid droplet size (**Supplementary Figure S10G-J**).

Metabolic phenotyping and behavioral analysis revealed comparable overall energy expenditure and oxygen consumption between AL and CR mice (**Supplementary Figure S10K-N**). However, carbon dioxide production and carbohydrate oxidation were higher in CR mice during the dark period when food was available (**Supplementary Figure S10O-R**), indicating a higher preference for carbohydrate metabolism in CR mice during active feeding periods and a rapid shift towards fatty acid metabolism during inactivity and food withdrawal. To assess how CR influences glucose homeostasis in aged mice, we performed mixed meal tolerance tests (MTTs; 2 g glucose/kg body weight). Baseline MTTs were conducted at 72 weeks, prior to CR. After 2 months of CR, old mice exhibited significantly improved glucose tolerance at 80 weeks, attributed to enhanced insulin sensitivity (**Figure 6C**). This improvement was accompanied by ~50% reductions in fasting and glucose-stimulated beta cell insulin secretion (**Supplementary Figure S10S**). This indicates that CR preserves aging beta cell function by reducing the relative insulin secretory demand required to maintain normoglycemia, demonstrating that known CR-mediated functional beta cell adaptation (*33*) remains intact in aging (**Supplementary Figure S10T**).

We previously showed that CR modulates beta cell heterogeneity by activating pro-longevity and pro-homeostasis transcriptional mechanisms that enhance beta cell protein and organelle quality-control mechanisms (*33*). This transcriptional response is driven by the activation of TF-directed GRNs that increase the expression of beta cell identity and longevity genes (*33*). Therefore, to determine whether CR elicits similar adaptative programs to old beta cells during CR, we performed single nucleus RNA sequencing (snRNA-seq, 10X genomics) on islet nuclei isolated from AL and CR-fed mice (**Figure 6A**). A total of 32,380 cells were sequenced (AL=17,344, CR=15,306) to identify all major islet cell types, including beta cells (*Ins1*, *Ins2*, and *Ero1b*), alpha cells (*Gcg*), delta cells (*Sst*), endothelial cells (*Pecam1*), and pancreatic polypeptide cells (*Ppy*) (**Figure 6D-E, Supplementary Figure S11A**). Approximately 65% of the sequenced cells were beta cells, and CR did not impact the relative composition of the heterogeneous beta cell population or islet cytoarchitecture composition (**Supplementary Figure S11B-D**). Using pseudobulk analysis of beta cells followed by KEGG and STRING databases, we observed a narrow range of CR-mediated effects on beta cell gene expression, limited to downregulation of few ER protein processing and folding (*Hspa1a/b/HSP70, Hspa8, Hsp90ab1, Dnaja1/HSP40, and Calr)*, cell stress (*Ypel2*, *Txnip*), and insulin synthesis (*Ins1*) genes (**Figure 6F and Supplementary Figure S11E-J**). These data indicate that CR has a very limited impact on beta cell transcriptional programs in aged mice despite a significant downregulation of insulin release *in vivo*.

Remarkably, CR exerted a stronger transcriptional effect on alpha cells, modulating nearly five times more genes than beta cells (184 vs. 36 differentially expressed genes; **Figure 6F, Supplementary Table S15**). Differential gene expression and pathway enrichment analyses of old CR alpha cell gene signatures revealed upregulation of pathways associated with glucagon, glucose and fatty acid metabolism (*Gcg, Gys2, Acacb*, and *Pgc1a*/*Ppargc1a)* (**Figure 6G**). In contrast, CR suppressed 159 genes involved in TCR signaling, antigen presentation, and

348 immune cell recruitment pathways *(***Figure 6H, Supplement Figure S12**). This included genes
349 involved in cell-cell signaling via MHC class I (H2-D1, *H2-Q7*, *H2-Q6*, *H2-K1*) and some MHC
350 class II (*H2-Aa*, *H2-Ab1*) antigens **(Figure 6H-I)**. Because MHC-I antigens is more prominent in
351 islet endocrine cells than MHC-II, we constructed an MHC-I module score based on heavy and
352 light chain genes (*H2-K1, H2-D1, H2-Q2, H2-Q5,H2-Q6,H2-Q7,H2-Q12*) detected in our
353 scRNA-seq data, and found the module score was reduced by CR (**Figure 6J**).

354 Taken together, these findings demonstrate that 2 months of CR reduces pro-inflamma-
355 tory signaling in aging alpha cells in mice, and it induces a state of beta cell rest that does not
356 involve significant changes to beta cell transcriptional mechanisms.

357 **CR suppresses alpha cell immune signaling to reduce islet inflammation.** To further inves-
358 tigate how CR-mediated modulation of aging alpha cell inflammatory gene expression influ-
359 ences the cellular and molecular profile of islet immune cells, we quantified the relative compo-
360 sition and transcriptional signatures immune cell types identified by snRNA-seq (**Figure 7A**).
361 This revealed a significant decrease in B cells, T cells, proliferating B cells, and antigen present-
362 ing cells (APCs) in CR mouse islets, whereas the relative density and transcriptional profile of
363 islet-resident macrophages were unchanged (**Figure 7B**). Old CR mouse islets had a marked
364 reduction in islet T cells, including a near total ablation of cytotoxic $CD8^+$ effector T cells (**Figure**
365 **7C-D**). In addition, the remaining $CD8^+$ T cells in CR islets had reduced expression of effector
366 markers granzyme K (*Gzmk*), IL-2 receptor (Il2ra/*Cd25*), Ccr7, and *Txk*; all markers of activated
367 $CD8^+$ T cells (**Figure 7E**). We validated these changes *in situ* using immunohistochemistry and
368 confocal microscopy of AL and CR old pancreases, followed by spatial mapping of alpha cells,
369 beta cells, and $CD3^+$ T cells (**Figure 7F)**. This approach revealed a significant reduction in T-cell
370 density (**Figure 7G**), and increased distance between T cells and alpha cells (**Figure 7H**). The
371 proportion of T cells in proximity (within 6μm) to alpha cells trended higher (p=0.07), whereas
372 this enrichment was not observed for beta cells (**Supplementary Figure S13A-B**). Total macro-
373 phage content in proximity to islets was not altered by CR (**Supplementary Figure 13C-E**), and
374 the relative proportions of pro-inflammatory (M1-like) and anti-inflammatory (M2-like) macro-
375 phages were likewise unchanged (**Supplementary Figure S13F-K**). These data support recent
376 findings of immune cell infiltration in the aging mouse islet (*70*) and demonstrate that CR modu-
377 lates the recruitment of $CD8^+$ T cells to the islet by reducing their preferential proximity to old al-
378 pha cells.

379 To identify communication pathways linking aged alpha cells with $CD8^+$ T cells and their
380 modulation by CR, we performed receptor-ligand inference analysis using CellChat (*71, 72*) to
381 reconstruct cell-cell communication networks in islets from AL and CR mice (*73*). This analysis
382 revealed a downregulation of intercellular signaling between islet immune cells and endocrine
383 cell types, including alpha, beta, and delta cells (**Supplementary Figure S14A**). This was un-
384 derscored by a significant decrease in CD45-based interactions between old alpha cells and T-
385 and B-cells in CR mice (**Figure 7I**), accompanied by reduced complement signaling, particularly
386 toward T cells (**Figure 7J**). Moreover, CR attenuated T cell co-stimulation, as evidenced by re-
387 duced CD80 signaling from APCs and reduced CD86 signaling from B cells to T cells (**Supple-**
388 **mentary Figure S14B–C**). Chemokine signaling via CCL and CXCL pathways towards T cells
389 was similarly reduced under CR (**Supplementary Figure S14D-E**).

390 Overall, these results indicate that CR profoundly remodels the aging islet immune envi-
391 ronment by suppressing alpha cell inflammatory and MHC-I signaling, thereby reducing $CD8^+$ T
392 cell recruitment and cytotoxicity, and diminishing intercellular communication between alpha
393 cells and adaptive immune populations.

394 **<u>Discussion</u>**

395 Aging is associated with an active and low-grade inflammatory process in different tis-
396 sues, where inflammation is a key signature of several age-associated degenerative and meta-
397 bolic diseases, including Alzheimer's (*74*), and obesity and diabetes (*75*). In the pancreas, aging
398 is associated with increased islet macrophage infiltration and vascular fibrosis (*38*), and share
399 other key hallmarks of T1D and T2D islet pathophysiology such as beta cell ER stress, compro-
400 mised beta cell identity and function, and beta cell senescence (*15, 38, 39, 43-45, 56, 57, 76-*
401 *82*). Importantly, recent studies have implicated the activation of inflammatory responses in hu-
402 man alpha cells during T1D and T2D (*83, 84*).

403 Here, we identified the activation of immune signaling and inflammation as a key signa-
404 ture of aging human islets from non-diabetic individuals. This phenotype is defined by active
405 IFNγ signaling and MHC-I expression in old alpha cells due to activation of IFNγ-responsive TFs
406 IRF1, NFKB1, and STAT1. Activation of alpha cell immune signaling during aging translates into
407 increased physical interactions between old alpha cells with pancreas $CD8^+$ T cells, which accu-
408 mulate in the human islet microenvironment during aging. Strikingly, most old islet $CD8^+$ cells
409 have a "memory-like" phenotype ($CD27^+$), thus indicating that these cells have been exposed to
410 T cell antigens. While our study does not identify which antigen is presented by alpha cell MHC-
411 Is, a recent study where human islets were exposed to cytokine stress (e.g., IFNγ) identified
412 several new MHC-I antigens, many of which are enriched in aging alpha cells (i.e., NFKB1,
413 IRF9, TAP1, IFIT3, PSMB8, and STAT1)(*76*).

414 This aging alpha cell inflammatory phenotype correlates with an increase in the expres-
415 sion of several AA catabolism enzymes. This could explain the observed increase in amino-acid-
416 dependent glucagon release from isolated human islets and the elevated levels of glucagon in
417 old ND humans after a meal (*2*). Notably, elevated glucagon secretion after a mixed meal and
418 AA infusions is also observed in adults with T2D (*19-21*), thus suggesting that alpha cell inflam-
419 mation could also play a role during T2D pathogenesis. In fact, while we did not observe
420 changes in the density of islet CD8+ cells between ND and T2D islets, most T2D islet $CD8^+$
421 cells have an effector-like signature ($CD45RA^+CD8^+$). This suggests that infiltration of $CD8^+$ cells
422 in aging human islets occurs independently of T2D and further suggests that islet inflammation
423 in individuals with T2D onset during old age involves activation of alpha cell-interacting and "res-
424 ident" $CD8^+$ cells and broad islet inflammation signatures (*38, 80*).

425 In species spanning from yeast to humans, CR has been shown to extend lifespan and
426 health span (*32, 68, 69, 85-87*). The benefits of CR depend on improvements in glucose home-
427 ostasis, enhanced insulin sensitivity, and reduced metabolic demand for insulin release from
428 beta cells leading to beta cell rest (*33, 69, 88, 89*). In addition, CR can reduce overall inflamma-
429 tion signatures in different models, including humans (*32*). Our experiments with 80-week-old
430 mice on CR for 2 months demonstrate that the insulin-sensitizing and beta cell functional adap-
431 tation pathways promoted by CR are not impaired during aging and that these adaptations do
432 not require significant transcriptional reorganization. This is likely explained by the limited plas-
433 ticity of aging beta cells to respond to metabolic challenges (*90*), however the mechanisms un-
434 derlying this limited plasticity remain unknown. Notably, a recent study has shown that aging of
435 mouse endocrine islet cells is linked to immune activation and MHC-I gene expression (*82*).
436 While we did not observe this signature in aging beta cells and delta cells, CR acted on old al-
437 pha cells to significantly suppress the expression of pro-inflammatory genes, including MHC-I
438 signaling pathways. This CR-dependent modulation dampened CD45-mediated communication
439 between immune cells and alpha cells, which was sufficient to reduce the density of T cells in
440 aging islet periphery.

441 In conclusion, our findings identify the relationship between alpha cells and immune cells
442 within the islet of Langerhans during aging that may underlie pro-inflammatory injury and pro-
443 mote T2D development during old age.

Data availability: All source data and metadata, including IMC, CODEX, snRNA-seq, and source code data are publicly available and can be downloaded from Zenodo (10.5281/zenodo.17874622). Human islet single cell RNAseq uniformly reprocessed is available via PanKbase Zenodo (https://zenodo.org/records/15596314). Raw FASTQ data from mouse islet sequencing data are deposited at Gene Expression Omnibus and processed data is available on Github and Zenodo.

Acknowledgements: We acknowledge the following Vanderbilt University (VU) and Vanderbilt University Medical Center (VUMC) core facilities: VUMC Hormone Assay & Analytical Services Core (NIH DK020593), VU Metabolic Mouse Phenotyping Center [VMMPC (NIH DK059637; www.vmmpc.org)], Translational Pathology Shared Resource (NCI/NIH Cancer Center Support Grant 5P30 CA68485-19), and Vanderbilt Technologies for Advanced Genomics (VANTAGE) core laboratory. VANTAGE is supported in part by Clinical and Translational Science Award Grant 5UL1 RR024975-03, Vanderbilt Ingram Cancer Center Grant P30 CA68485, Vanderbilt Vision Center Grant P30 EY08126, and National Institutes of Health/National Center for Research Resources Grant G20 RR030956. This manuscript used data acquired from the database (https://hpap.pmacs.upenn.edu/) of the Human Pancreas Analysis Program (HPAP; RRID:SCR_016202)(*60, 61*). HPAP is part of a Human Islet Research Network (RRID:SCR_014393) consortium (UC4-DK112217, U01-DK123594, UC4-DK112232, and U01-DK123716). This work includes data and/or analyses from HumanIslets.com funded by the Canadian Institutes of Health Research, JDRF Canada, and Diabetes Canada (5-SRA-2021-1149-S-B/TG 179092) with data from islets isolated by the Alberta Diabetes Institute IsletCore with the support of the Human Organ Procurement and Exchange program, Trillium Gift of Life Network, BC Transplant, Quebec Transplant, and other Canadian organ procurement organizations with written informed donor consent as approved by the Human Research Ethics Board at the University of Alberta (Pro00013094). we would like to acknowledge Dr Patrick E MacDonald from ADI – Edmonton (Canada) for critical comments and inputs during data collection and manuscript writing stages of this project. We would also like to acknowledge NIH grant R01AG040178.

Funding: This work was support by the National Institutes of Health (NIH) grant R01DK138141 to R.A.D. M.S. is supported by the NIH Molecular Endocrinology Training Program (T32DK007563) and the American Diabetes Association (1-26-PDF-1109). A.C. was supported by an American Heart Association Postdoctoral Fellowship (26POST1571444).

Author Contributions: M.S., S.S., JP.C., and R.A.D designed experiments. M.S., A.C., M.C., G.F., S.S., JP.C., A.H., C.E., A.P., and R.A.D. collected data and assisted with data analysis and project management. M.S., S.S., JP.C., and R.A.D. completed data analysis. M.S. and R.A.D. interpreted data and wrote the manuscript.

Disclosures: The authors have nothing to disclose.

483 **REFERENCES**

484 1. National Diabetes Statistics Report. *Centers for Disease Control and Prevention*, (2024).
485 2. R. Basu *et al.*, Mechanisms of the age-associated deterioration in glucose tolerance:
486 contribution of alterations in insulin secretion, action, and clearance. *Diabetes* **52**, 1738-
487 1748 (2003).
488 3. K. F. Petersen *et al.*, Mitochondrial dysfunction in the elderly: possible role in insulin
489 resistance. *Science* **300**, 1140-1142 (2003).
490 4. C. C. Cowie *et al.*, Prevalence of diabetes and impaired fasting glucose in adults in the U.S.
491 population: National Health And Nutrition Examination Survey 1999-2002. *Diabetes Care*
492 **29**, 1263-1268 (2006).
493 5. A. Alpert *et al.*, A clinically meaningful metric of immune age derived from high-dimensional
494 longitudinal monitoring. *Nat Med* **25**, 487-495 (2019).
495 6. C. Sportès *et al.*, Administration of rhIL-7 in humans increases in vivo TCR repertoire
496 diversity by preferential expansion of naive T cell subsets. *J Exp Med* **205**, 1701-1714 (2008).
497 7. M. L. Pekalski *et al.*, Postthymic expansion in human CD4 naive T cells defined by
498 expression of functional high-affinity IL-2 receptors. *J Immunol* **190**, 2554-2566 (2013).
499 8. X. Sun *et al.*, Longitudinal analysis reveals age-related changes in the T cell receptor
500 repertoire of human T cell subsets. *J Clin Invest* **132**, (2022).
501 9. O. Cabrera *et al.*, The unique cytoarchitecture of human pancreatic islets has implications
502 for islet cell function. *Proceedings of the National Academy of Sciences* **103**, 2334-2339
503 (2006).
504 10. M. Cnop *et al.*, The long lifespan and low turnover of human islet beta cells estimated by
505 mathematical modelling of lipofuscin accumulation. *Diabetologia* **53**, 321-330 (2010).
506 11. R. A. E. Drigo *et al.*, Age Mosaicism across Multiple Scales in Adult Tissues. *Cell Metabolism*
507 **30**, 343-+ (2019).
508 12. S. Perl *et al.*, Significant human beta-cell turnover is limited to the first three decades of life
509 as determined by in vivo thymidine analog incorporation and radiocarbon dating. *J Clin*
510 *Endocrinol Metab* **95**, E234-239 (2010).
511 13. C. López-Otín, M. A. Blasco, L. Partridge, M. Serrano, G. Kroemer, Hallmarks of aging: An
512 expanding universe. *Cell* **186**, 243-278 (2023).
513 14. S. Shrestha *et al.*, Aging compromises human islet beta cell function and identity by
514 decreasing transcription factor activity and inducing ER stress. *Science Advances* **8**,
515 eabo3932 (2022).
516 15. I. Sandovici *et al.*, Ageing is associated with molecular signatures of inflammation and type
517 2 diabetes in rat pancreatic islets. *Diabetologia* **59**, 502-511 (2016).
518 16. L. Li *et al.*, Defects in β-cell Ca2+ dynamics in age-induced diabetes. *Diabetes* **63**, 4100-
519 4114 (2014).
520 17. G. M. Reaven, Y. D. Chen, A. Golay, A. L. Swislocki, J. B. Jaspan, Documentation of
521 hyperglucagonemia throughout the day in nonobese and obese patients with noninsulin-
522 dependent diabetes mellitus. *J Clin Endocrinol Metab* **64**, 106-110 (1987).
523 18. K. Færch *et al.*, Insulin Resistance Is Accompanied by Increased Fasting Glucagon and
524 Delayed Glucagon Suppression in Individuals With Normal and Impaired Glucose
525 Regulation. *Diabetes* **65**, 3473-3481 (2016).
526 19. R. H. Unger, E. Aguilar-Parada, W. A. Müller, A. M. Eisentraut, Studies of pancreatic alpha
527 cell function in normal and diabetic subjects. *J Clin Invest* **49**, 837-848 (1970).
528 20. D. D'Alessio, The role of dysregulated glucagon secretion in type 2 diabetes. *Diabetes Obes*
529 *Metab* **13 Suppl 1**, 126-132 (2011).

21. P. Raskin, I. Aydin, T. Yamamoto, R. H. Unger, Abnormal alpha cell function in human diabetes: the response to oral protein. *Am J Med* **64**, 988-997 (1978).
22. P. Raskin, I. Aydin, R. H. Unger, Effect of insulin on the exaggerated glucagon response to arginine stimulation in diabetes mellitus. *Diabetes* **25**, 227-229 (1976).
23. L. Fontana, L. Partridge, V. D. Longo, Extending healthy life span--from yeast to humans. *Science* **328**, 321-326 (2010).
24. J. A. Mattison *et al.*, Caloric restriction improves health and survival of rhesus monkeys. *Nat Commun* **8**, 14063 (2017).
25. C. L. Green, D. W. Lamming, L. Fontana, Molecular mechanisms of dietary restriction promoting health and longevity. *Nat Rev Mol Cell Biol* **23**, 56-73 (2022).
26. R. M. Anderson, D. G. Le Couteur, R. de Cabo, Caloric Restriction Research: New Perspectives on the Biology of Aging. *J Gerontol A Biol Sci Med Sci* **73**, 1-3 (2017).
27. K. Mao *et al.*, Late-life targeting of the IGF-1 receptor improves healthspan and lifespan in female mice. *Nat Commun* **9**, 2394 (2018).
28. G. Y. Liu, D. M. Sabatini, mTOR at the nexus of nutrition, growth, ageing and disease. *Nat Rev Mol Cell Biol* **21**, 183-203 (2020).
29. D. Il'yasova *et al.*, Effects of 2 years of caloric restriction on oxidative status assessed by urinary F2-isoprostanes: The CALERIE 2 randomized clinical trial. *Aging Cell* **17**, (2018).
30. L. Yang, P. Li, S. Fu, E. S. Calay, G. S. Hotamisligil, Defective hepatic autophagy in obesity promotes ER stress and causes insulin resistance. *Cell Metab* **11**, 467-478 (2010).
31. J. O. Pyo *et al.*, Overexpression of Atg5 in mice activates autophagy and extends lifespan. *Nat Commun* **4**, 2300 (2013).
32. O. Spadaro *et al.*, Caloric restriction in humans reveals immunometabolic regulators of health span. *Science* **375**, 671-+ (2022).
33. C. dos Santos *et al.*, Calorie restriction increases insulin sensitivity to promote beta cell homeostasis and longevity in mice. *Nature Communications* **15**, 9063 (2024).
34. L. Matta *et al.*, Chronic intermittent fasting impairs β cell maturation and function in adolescent mice. *Cell Rep* **44**, 115225 (2025).
35. S. Patel, Z. Yan, M. S. Remedi, Intermittent fasting protects β-cell identity and function in a type-2 diabetes model. *Metabolism* **153**, 155813 (2024).
36. M. R. Brown *et al.*, Time-restricted feeding prevents deleterious metabolic effects of circadian disruption through epigenetic control of β cell function. *Sci Adv* **7**, eabg6856 (2021).
37. L. Mateus Gonçalves, E. Pereira, J. P. Werneck de Castro, E. Bernal-Mizrachi, J. Almaça, Islet pericytes convert into profibrotic myofibroblasts in a mouse model of islet vascular fibrosis. *Diabetologia* **63**, 1564-1575 (2020).
38. J. Almaca *et al.*, Young capillary vessels rejuvenate aged pancreatic islets. *Proceedings of the National Academy of Sciences of the United States of America* **111**, 17612-17617 (2014).
39. J. J. Wright *et al.*, Exocrine Pancreas in Type 1 and Type 2 Diabetes: Different Patterns of Fibrosis, Metaplasia, Angiopathy, and Adiposity. *Diabetes* **73**, 1140-1152 (2024).
40. J. D. Ewald *et al.*, HumanIslets.com: Improving accessibility, integration, and usability of human research islet data. *Cell Metab* **37**, 7-11 (2025).
41. J. Kolic *et al.*, Proteomic predictors of individualized nutrient-specific insulin secretion in health and disease. *Cell Metab* **36**, 1619-1633.e1615 (2024).
42. J. Camunas-Soler *et al.*, Patch-Seq Links Single-Cell Transcriptomes to Human Islet Dysfunction in Diabetes. *Cell Metabolism* **31**, 1017-+ (2020).

43. C. Aguayo-Mazzucato *et al.*, Acceleration of beta Cell Aging Determines Diabetes and Senolysis Improves Disease Outcomes. *Cell Metabolism* **30**, 129-+ (2019).
44. S. Shrestha *et al.*, Aging compromises human islet beta cell function and identity by decreasing transcription factor activity and inducing ER stress. *Science Advances* **8**, 17 (2022).
45. M. Enge *et al.*, Single-Cell Analysis of Human Pancreas Reveals Transcriptional Signatures of Aging and Somatic Mutation Patterns. *Cell* **171**, 321-330.e314 (2017).
46. S. Tritschler, F. J. Theis, H. Licked, A. Bottcher, Systematic single-cell analysis provides new insights into heterogeneity and plasticity of the pancreas. *Molecular Metabolism* **6**, 974-990 (2017).
47. P. Augsornworawat, K. G. Maxwell, L. Velazco-Cruz, J. R. Millman, Single-Cell Transcriptome Profiling Reveals β Cell Maturation in Stem Cell-Derived Islets after Transplantation. *Cell Rep* **32**, 108067 (2020).
48. J. Chiou *et al.*, Single-cell chromatin accessibility identifies pancreatic islet cell type- and state-specific regulatory programs of diabetes risk. *Nature Genetics* **53**, 455-+ (2021).
49. N. C. Bramswig *et al.*, Epigenomic plasticity enables human pancreatic α to β cell reprogramming. *J Clin Invest* **123**, 1275-1284 (2013).
50. D. Avrahami *et al.*, Aging-Dependent Demethylation of Regulatory Elements Correlates with Chromatin State and Improved β Cell Function. *Cell Metabolism* **22**, 619-632 (2015).
51. D. Avrahami *et al.*, Single-cell transcriptomics of human islet ontogeny defines the molecular basis of β-cell dedifferentiation in T2D. *Mol Metab* **42**, 101057 (2020).
52. C. Su *et al.*, 3D chromatin maps of the human pancreas reveal lineage-specific regulatory architecture of T2D risk. *Cell Metabolism* **34**, 1394-+ (2022).
53. H. E. Arda *et al.*, Age-Dependent Pancreatic Gene Regulation Reveals Mechanisms Governing Human beta Cell Function. *Cell Metabolism* **23**, 909-920 (2016).
54. M. Fasolino *et al.*, Single-cell multi-omics analysis of human pancreatic islets reveals novel cellular states in type 1 diabetes. *Nature Metabolism* **4**, 284-+ (2022).
55. A. R. Patil *et al.*, Single-cell expression profiling of islets generated by the Human Pancreas Analysis Program. *Nat Metab* **5**, 713-715 (2023).
56. C. Aguayo-Mazzucato *et al.*, beta Cell Aging Markers Have Heterogeneous Distribution and Are Induced by Insulin Resistance. *Cell Metabolism* **25**, 898-+ (2017).
57. P. J. Thompson *et al.*, Targeted Elimination of Senescent Beta Cells Prevents Type 1 Diabetes. *Cell Metab* **29**, 1045-1060.e1010 (2019).
58. B. van de Sande *et al.*, A scalable SCENIC workflow for single-cell gene regulatory network analysis. *Nature Protocols* **15**, 2247-2276 (2020).
59. A. N. Schep, B. Wu, J. D. Buenrostro, W. J. Greenleaf, chromVAR: inferring transcription-factor-associated accessibility from single-cell epigenomic data. *Nat Methods* **14**, 975-978 (2017).
60. K. H. Kaestner, A. C. Powers, A. Naji, M. A. Atkinson, NIH Initiative to Improve Understanding of the Pancreas, Islet, and Autoimmunity in Type 1 Diabetes: The Human Pancreas Analysis Program (HPAP). *Diabetes* **68**, 1394-1402 (2019).
61. S. N. Shapira, A. Naji, M. A. Atkinson, A. C. Powers, K. H. Kaestner, Understanding islet dysfunction in type 2 diabetes through multidimensional pancreatic phenotyping: The Human Pancreas Analysis Program. *Cell Metab* **34**, 1906-1913 (2022).
62. É. Korpos *et al.*, Identification and characterisation of tertiary lymphoid organs in human type 1 diabetes. *Diabetologia* **64**, 1626-1641 (2021).
63. M. H. Wu *et al.*, Single-cell analysis of the human pancreas in type 2 diabetes using multi-spectral imaging mass cytometry. *Cell Reports* **37**, 15 (2021).

625 64. Y. J. Wang *et al.*, Multiplexed In Situ Imaging Mass Cytometry Analysis of the Human
626 Endocrine Pancreas and Immune System in Type 1 Diabetes. *Cell Metab* **29**, 769-783.e764
627 (2019).
628 65. C. Talchai, S. H. Xuan, H. V. Lin, L. Sussel, D. Accili, Pancreatic beta Cell Dedifferentiation as
629 a Mechanism of Diabetic beta Cell Failure. *Cell* **150**, 1223-1234 (2012).
630 66. C. Dos Santos *et al.*, Caloric restriction promotes beta cell longevity and delays aging and
631 senescence by enhancing cell identity and homeostasis mechanisms. *Res Sq*, (2023).
632 67. E. Duregon *et al.*, Prolonged fasting times reap greater geroprotective effects when
633 combined with caloric restriction in adult female mice. *Cell Metab* **35**, 1179-1194.e1175
634 (2023).
635 68. S. J. Mitchell *et al.*, Effects of Sex, Strain, and Energy Intake on Hallmarks of Aging in Mice.
636 *Cell Metabolism* **23**, 1093-1112 (2016).
637 69. H. H. Pak *et al.*, Fasting drives the metabolic, molecular and geroprotective effects of a
638 calorie-restricted diet in mice. *Nature Metabolism* **3**, 1327-+ (2021).
639 70. S. Jin *et al.*, Inference and analysis of cell-cell communication using CellChat. *Nat Commun*
640 **12**, 1088 (2021).
641 71. A. Coomans de Brachène *et al.*, Exercise as a non-pharmacological intervention to protect
642 pancreatic beta cells in individuals with type 1 and type 2 diabetes. *Diabetologia* **66**, 450-
643 460 (2023).
644 72. P. Carapeto *et al.*, Exercise activates AMPK in mouse and human pancreatic islets to
645 decrease senescence. *Nature Metabolism*, (2024).
646 73. H. Al Jobori *et al.*, Empagliflozin Treatment Is Associated With Improved β-Cell Function in
647 Type 2 Diabetes Mellitus. *J Clin Endocrinol Metab* **103**, 1402-1407 (2018).
648 74. C. M. Kellogg *et al.*, Microglial MHC-I induction with aging and Alzheimer's is conserved in
649 mouse models and humans. *Geroscience* **45**, 3019-3043 (2023).
650 75. S. SantaCruz-Calvo *et al.*, Adaptive immune cells shape obesity-associated type 2 diabetes
651 mellitus and less prominent comorbidities. *Nat Rev Endocrinol* **18**, 23-42 (2022).
652 76. P. P. Nanaware *et al.*, The antigen presentation landscape of cytokine-stressed human
653 pancreatic islets. *Cell Rep* **44**, 115927 (2025).
654 77. L. Marselli *et al.*, beta-Cell inflammation in human type 2 diabetes and the role of
655 autophagy. *Diabetes Obesity & Metabolism* **15**, 130-136 (2013).
656 78. J. Jelleschitz *et al.*, Insulitis and aging: Immune cell dynamics in Langerhans islets. *Redox*
657 *Biol* **82**, 103587 (2025).
658 79. M. De Burghgrave *et al.*, Pancreatic Islet Cells Response to IFNγ Relies on Their Spatial
659 Location within an Islet. *Cells* **12**, (2022).
660 80. D. Avrahami *et al.*, Single-cell transcriptomics of human islet ontogeny defines the
661 molecular basis of beta-cell dedifferentiation in T2D. *Molecular Metabolism* **42**, 14 (2020).
662 81. E. Horwitz *et al.*, β-Cell DNA Damage Response Promotes Islet Inflammation in Type 1
663 Diabetes. *Diabetes* **67**, 2305-2318 (2018).
664 82. W. Staels *et al.*, Comprehensive alpha, beta, and delta cell transcriptomics reveal an
665 association of cellular aging with MHC class I upregulation. *Mol Metab* **87**, 101990 (2024).
666 83. T. Dos Santos *et al.*, Altered immune and metabolic molecular pathways drive islet cell
667 dysfunction in human type 1 diabetes. *J Clin Invest*, (2025).
668 84. X. Q. Dai *et al.*, Heterogenous impairment of alpha cell function in type 2 diabetes is linked
669 to cell maturation state. *Cell Metabolism* **34**, 256-+ (2022).
670 85. V. D. Longo, R. M. Anderson, Nutrition, longevity and disease: From molecular mechanisms
671 to interventions. *Cell* **185**, 1455-1470 (2022).

86. J. A. Mattison *et al.*, Impact of caloric restriction on health and survival in rhesus monkeys from the NIA study. *Nature* **489**, 318-321 (2012).
87. A. E. Civitarese *et al.*, Calorie restriction increases muscle mitochondrial biogenesis in healthy humans. *PLoS Med* **4**, e76 (2007).
88. M. E. C. da Amaral *et al.*, Caloric restriction recovers impaired beta-cell-beta-cell gap junction coupling, calcium oscillation coordination, and insulin secretion in prediabetic mice. *American Journal of Physiology-Endocrinology and Metabolism* **319**, E709-E720 (2020).
89. C. J. Sheng *et al.*, Reversibility of beta-Cell-Specific Transcript Factors Expression by Long-Term Caloric Restriction in db/db Mouse. *Journal of Diabetes Research* **2016**, 11 (2016).
90. S. I. Tschen, S. Dhawan, T. Gurlo, A. Bhushan, Age-dependent decline in beta-cell proliferation restricts the capacity of beta-cell regeneration in mice. *Diabetes* **58**, 1312-1320 (2009).
91. M. E. Ritchie *et al.*, limma powers differential expression analyses for RNA-sequencing and microarray studies. *Nucleic acids research* **43**, e47-e47 (2015).
92. M. I. Love, W. Huber, S. Anders, Moderated estimation of fold change and dispersion for RNA-seq data with DESeq2. *Genome Biol* **15**, 550 (2014).
93. Y. Hao *et al.*, Dictionary learning for integrative, multimodal and scalable single-cell analysis. *Nat Biotechnol* **42**, 293-304 (2024).
94. Y. J. Wang *et al.*, Single-Cell Mass Cytometry Analysis of the Human Endocrine Pancreas. *Cell Metabolism* **24**, 616-626 (2016).
95. R. J. Colman *et al.*, Caloric restriction delays disease onset and mortality in rhesus monkeys. *Science* **325**, 201-204 (2009).

696 **Figure Legends**

697 **Figure 1 - Aging human islets have an inflammatory activation phenotype combined with**
698 **mTORC1 signaling and elevated unfolded protein response stress. (A)** Islets from young
699 (28±4 years, n=26), and old (71±3 years, n=19) ND donors from the HumanIslets consortium
700 were compared by proteomics meta-analysis. **(B)** Reactome pathways present from significantly
701 abundant proteins between young and old ND donors. **(C-G)** Protein expression levels for beta
702 cell immaturity marker, RBP4 (C); senescence, CDKN1A/p21 (D); unfolded protein response,
703 CHOP (DDIT3), ATF6, PERK (EIF2AK3) (E); mTORC1 activation, LAMP2, LAMTOR, RAGA,
704 RAGC (F); and immune regulatory components, HLA-A, TGF-β1, TOM1, CD63, CD44, and
705 CD28, respectively (G). HLA, human leukocyte antigen. *p<0.05, young vs. old donors. Error
706 bars are mean ± SD.

707 **Figure 2 - Aging increases human alpha cell interferon signaling and metabolic signa-**
708 **tures. (A)** Cell type UMAP of integrated scRNA-seq data obtained from HPAP database. **(B)**
709 Heatmap with hierarchical clustering showing top 25 genes differentially regulated by age in hu-
710 man alpha cells. **(C)** GSEA hallmarks for gene sets associated with the Hallmark Interferon
711 GAMMA Response (M5913). **(D)** Relative gene expression levels of genes in the Hallmark Inter-
712 feron GAMMA Response (M5913) collection in alpha cells versus beta cells. Asterisks mark
713 genes significantly upregulated in either cell type. **(E)** Weighted KEGG pathway analysis
714 demonstrating the enrichment of IFN-γ associated genes in old alpha cells versus old beta cells.
715 **(F-G)** Significantly expressed Hallmark genes for metabolic processes including Glycolysis
716 (M5937; G) and Amino Acid Metabolic Process (GO:0006520), respectively. **(H-K)** Isolated hu-
717 man islet perifusion assay including stimulation with amino-acids, glucose, IBMX, and KCL. Dot-
718 ted line boxes and represented quantification (**I**, **J**, and **K**) highlight specific stimuli that provoked
719 significant glucagon secretion from old islets versus young islets. P-values are shown. Data are
720 mean ± SD with boxplots representing mean ± IQR. ND, non-diabetic. HPAP, Human Pancreas
721 Analysis Program; GSEA, gene set enrichment analysis.

722 **Figure 3 - Re-wiring of gene regulatory networks activates an interferon-stimulated in-**
723 **flammatory phenotype in aging alpha cells. (A)** Regulon specificity scores (RSS) ratios be-
724 tween old and young alpha cells, with enrichment defined as the top 10% of RSS ratios within
725 each group. **(B)** Annotated Gene Regulatory Network (GRN) maps of young (top) and old (bot-
726 tom) human alpha cells. Transcription factors (TFs) are represented by white hexagons and in-
727 ferred TF target genes are shown in solid grey circles. Only the top 15% TF regulons after 100X
728 pySCENIC inference simulations are shown. TF hexagon size represents the TF importance
729 metric within the GRN structure, and TF-target gene nodes are connected by line edges colored
730 using a *viridis* hue to represent predicted connection strength. Shaded blue boxes are anno-
731 tated with pathway enrichment terms associated with their respective regulon network. **(C)** Venn
732 diagrams representing unique and shared genes found in the regulons associated with IRF1,
733 NFKB1, STAT1, AND MAFB TFs. **(D)** Regulatory network map displaying age-dependent and
734 age-independent regulatory connections between inflammatory TFs and canonical alpha cell
735 identity TFs. In this map, TFs are represented by solid grey circles and regulatory relationships
736 are shown by arrows. Green arrows, connections found in both young and old alpha cells; dark
737 blue and beige arrows represent connections found uniquely in old and young alpha cells, re-
738 spectively. **(E)** Venn diagram illustrating the overlap between SCENIC and chromVAR associ-
739 ated TFs detected in old alpha cells.

740 **Figure 4 - Aging increases $CD8^+$ islet infiltration via alpha cell MHC-I signaling. (A)** Imag-
741 ing Mass Cytometry (IMC) UMAPs displaying subset pancreas cells from all donors, highlighting
742 the islet-endocrine cells (top) and immune cells (bottom). **(B)** Representative IMC images and
743 spatial reconstructions of islet-endocrine (top) and islet-immune (bottom) fractions. Scale bar =
744 100μm. **(C)** UMAPs of pancreas cell subpopulations, highlighting endocrine cells (top) and

immune subsets (bottom). **(D)** Representative CODEX images and spatial reconstructions for islet immune subpopulations. Scale bar = 2000µm. **(E)** Representative islet for an aged donor, displaying C-peptide (yellow), glucagon (green), CD45 (white) and CD8 (magenta), with inset illustrating alpha-CD8 T cell interaction. Scale bar; image = 100µm, inset = 10µm. **(F-G)** Immune cell proportions within the total pancreatic immune pool, collected by both IMC (F) and CODEX (H) imaging platforms. **(H)** Density plots illustrating networking distance between $CD8^+$ T cells distance and alpha cells, median $CD8^+$-alpha cell distance, and the percentage of alpha cells localized within ≤50µm of $CD8^+$ T cells. **(I)** Density plots showing network distance between $CD8^+$ T cells and beta cells, median $CD8^+$-beta cell distance, and the percentage of beta cells localized within ≤50µm of $CD8^+$ T cells. **(J)** Representative IMC images illustration alpha cells (GCG, red) beta cells (C-peptide, white), and scaled HLA-ABC expression. Scale bar = 100µm. **(K-L).** Quantification of HLA-ABC (K) and HLA-DR (L) intensity from segmented alpha cells and beta cells. IMC, imaging mass cytometry; CyTOF, Cytometry by time-of-flight; ROI, region of interest. Welch's two-sample *t-test* was used to compare young and old donors in panels F-G, H-I, and K-L. Data are mean ± SEM (panels F-I), median ± SEM (K-L).

Figure 5 - T2D expands pancreatic $CD8^+$ T-cell populations and shifts islet $CD8^+$ T-cell states from towards terminal effector-memory phenotypes. (A) Clinical characteristics ND and T2D adults included for HPAP CODEX imaging. **(B)** UMAP of integrated pancreas samples (942,724 cells) were segmented into immune cells (195,140 cells) and islet endocrine (99,744 cells) populations. **(C)** Identified islet endocrine cell populations, including alpha (GCG^+), beta ($C\text{-}PEP^+$), "fibrotic" beta cells ($C\text{-}PEP^+$, $COL4A1^+$, $COL6^+$), delta (SST^+), pancreatic polypeptide (PP^+), and epsilon ($ghrelin^+$) cells. **(D)** Scaled beta cell expression of C-PEP, CHGA, and NKX6-1. **(E)** Scaled alpha cell expression of SOX9. **(F)** Proportions of major pancreatic immune subsets, including M2-like macrophages ($CD163^+CD68^+$), M1-like macrophages ($CD68^+CD163^-$), granulocytes/monocytes ($CD66b^+$), $CD8^+$ T cells ($CD3^+CD8^+$), and $CD4^+$ T cells ($CD3^+CD4^+$). **(G)** Immune cell density expressed as cells per mm^2. **(H)** CyTOF analysis of islets isolated from young ND (n=12), old ND(n=15), and T2D (n=13) donors. **(I)** Representative gating of viable $CD45^+$ immune cells (left) and $CD3^+CD8^+$ T cells (right), sourced from HPAP-164. **(J)** Proportion of $CD45^+$ immune cells among viable islet cells (left) and $CD3^+CD8^+$ within the $CD45^+$ compartment (right). **(K)** Representative two-parameter (CD27 x CD45RA) plot illustrating $CD8^+$ T-cell differentiation states; (1) naïve $CD27^+CD45RA^+$, (2) central memory ($CD27^+CD45RA^-$), 3) and terminal effector memory ($CD27^-CD45RA^+$). **(L)** Distribution of $CD8^+$ T cells across naïve $CD27^+CD45RA^+$; $CD8_{naïve}$), central memory ($CD27^+CD45RA^-$; $CD8_{CM}$), and terminal effector memory ($CD27^-CD45RA^+$; $CD8_{TEM}$) phenotypes. **(M)** $CD8^+$ T_{EM}/T_{CM} ratio, representing the relative expansion of terminal effector-memory $CD8^+$ T cells compared with the central memory pool. Welch's two sample *t-test* was used for comparisons between pool ND and T2D donors in panels A and C-G. One-way *ANOVA* compared young, old and T2D donors in panels J and L-M. DC, dendritic cell; cDC1, conventional cell; PP, pancreatic polypeptide; NK, natural killer. *p< 0.05, **p<0.01 for age (old vs. young) and ND vs. T2D groups. Data are mean ± SEM.

Figure 6 - Late-life CR improves glucose tolerance while downregulating alpha cell TCR activation and antigen presentation and processing. (A) 72-week-old C57Bl/6J mice were fed ad-libitum (AL, control) or subjected to 20% calorie restriction (CR) for 2 months. Islets were collected at 80 weeks and processed for IHC and snRNA-seq. **(B)** Percent change in body weight relative to baseline. **(C)** MTTs were performed at baseline (72 weeks) and after the intervention (80 weeks). AUC is presented for each test before and after dietary intervention. **(D)** UMAP of 32,380 islet cells. **(E)** Selected marker genes for endocrine islet subpopulations by scaled gene expression and percent cell expression. **(F)** Number of DEGs affected by CR in endocrine/endothelial cell populations. **(G)** KEGG pathways significantly modified by CR in alpha cells. **(H)** Protein-protein interaction networks predicted from genes downregulated by CR in alpha cells, and subset by 'leukocyte activation' subcluster in red. **(I)** Scaled single-cell expression

795 of MHC class I in alpha cells. **(J)** Scaled expression UMAP and box plot showing relative MHC-I
796 module scores, derived from *H2-K1, H2-D1, H2-Q2, H2-Q5, H2-Q6, H2-Q7, and H2-Q12* genes,
797 in AL and CR alpha cells. AUC, area under curve; IHC, immunohistochemistry; MTT, mixed meal
798 tolerance test; snRNA-seq, single nucleus RNA sequencing. #p< 0.05 for dietary groups (AL vs.
799 CR); ****p<0.0001 for intervention (Pre- vs. Post-CR).

800 **Figure 7 - Late-life CR attenuates islet adaptive CD8$^+$ effector phenotypes and reduces al-**
801 **pha cell-mediated T-cell recruitment. (A)** UMAP of subset immune cell populations (B cells, T
802 cells, macrophages, proliferating B cells, and APCs [dendritic cells] from AL and CR groups. **(B)**
803 Proportion of immune cell populations relative to total islet cells. **(C)** UMAP of T-cell populations
804 from AL and CR groups. **(D)** Proportion of total T cells; * denotes effector CD8$^+$ T cells. **(E)** Ex-
805 pression of Th1-associated genes: *Gzmk*, *Cd25/Il2ra*, *CCr7*, and *Txk*. **(F)** Representative IHC
806 staining for alpha cells (glucagon, red), beta cells (insulin, green) and T cells (CD3, purple).
807 Scale bar = 100µm. **(G)** Pancreatic T-cell density (CD3$^+$ T-cell counts per mm^2). **(H)** T-cell-endo-
808 crine cell networks, quantifying the average distance of CD3$^+$ T cells to alpha cells (left), and
809 beta cells (right). **(I-J)** Intercellular communication networks showing inferred CD45 signaling
810 and complement signaling interactions, respectively.

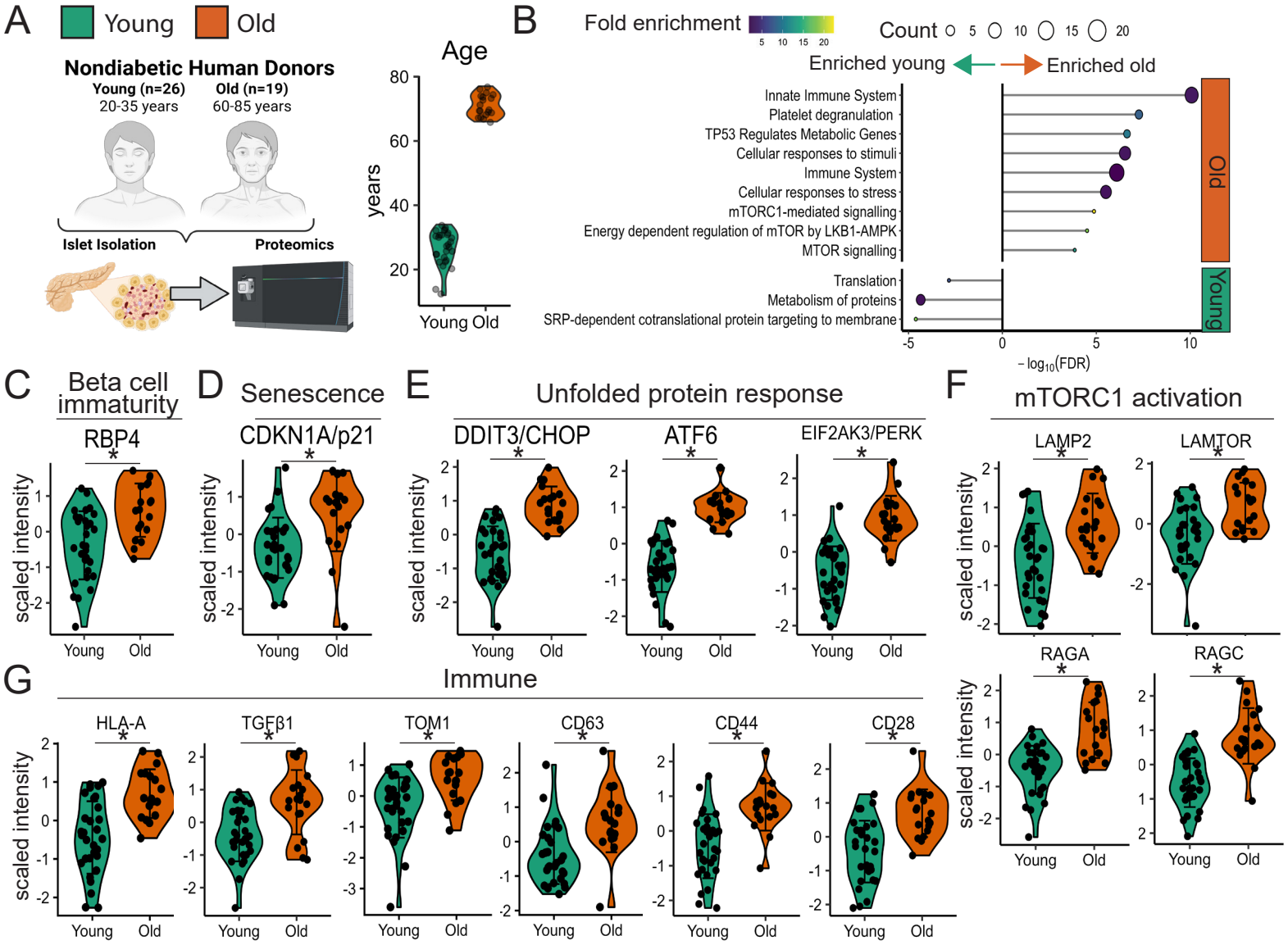
A
Young
Old
Nondiabetic Human Donors
Young (n=26)
20-35 years
Old (n=19)
60-85 years
Islet Isolation
Proteomics
Age
years
Young Old
B
Fold enrichment
Count
Enriched young
Enriched old
Innate Immune System
Platelet degranulation
TP53 Regulates Metabolic Genes
Cellular responses to stimuli
Immune System
Cellular responses to stress
mTORC1-mediated signalling
Energy dependent regulation of mTOR by LKB1-AMPK
MTOR signalling
Translation
Metabolism of proteins
SRP-dependent cotranslational protein targeting to membrane
Old
Young
$-\log_{10}$(FDR)
C
Beta cell immaturity
RBP4
D
Senescence
CDKN1A/p21
E
Unfolded protein response
DDIT3/CHOP
ATF6
EIF2AK3/PERK
F
mTORC1 activation
LAMP2
LAMTOR
RAGA
RAGC
G
Immune
HLA-A
TGFβ1
TOM1
CD63
CD44
CD28
scaled intensity
Young
Old

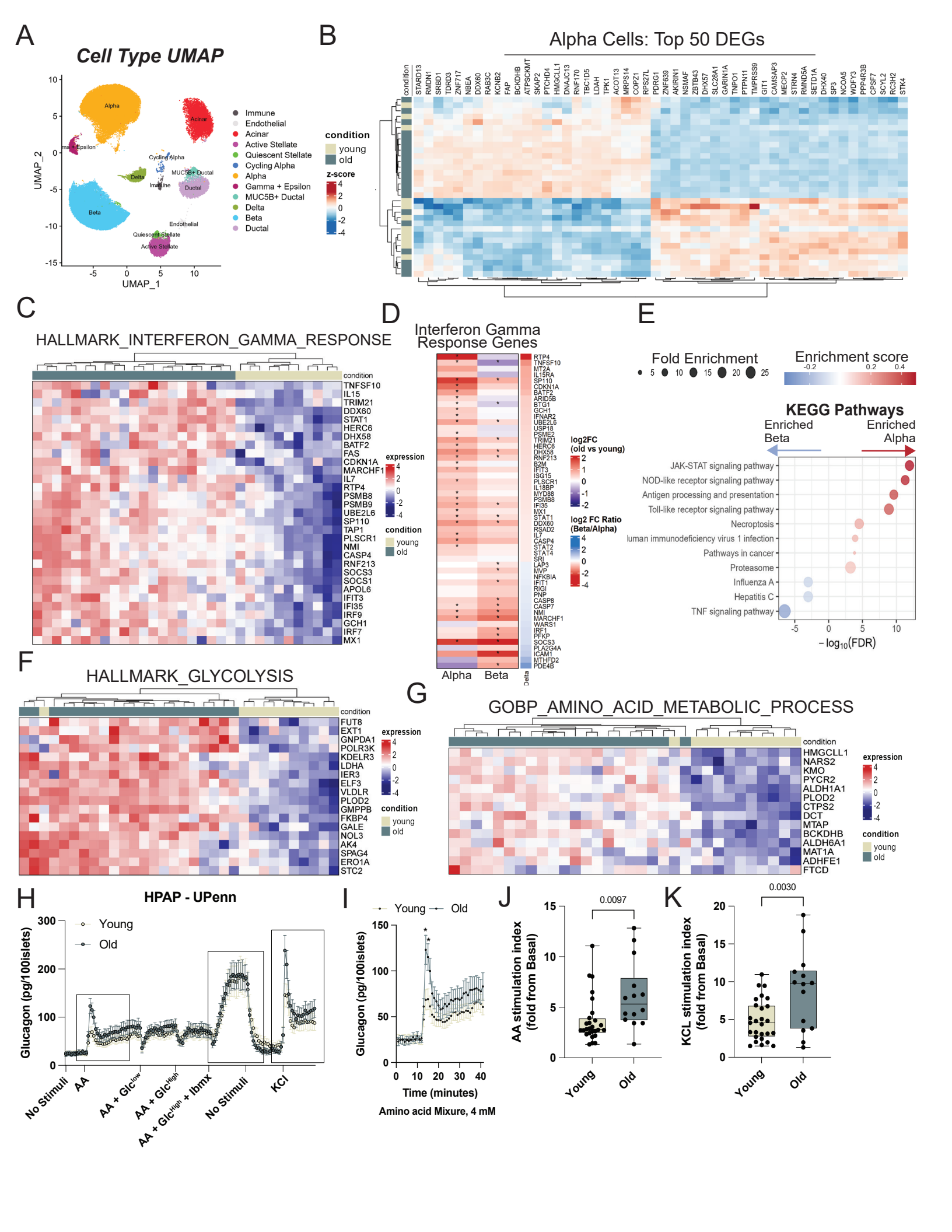
A
Cell Type UMAP
UMAP_1
UMAP_2
Alpha
Acinar
Gamma + Epsilon
Cycling Alpha
MUC5B+ Ductal
Delta
Immune
Ductal
Beta
Endothelial
Quiescent Stellate
Active Stellate
Immune
Endothelial
Acinar
Active Stellate
Quiescent Stellate
Cycling Alpha
Alpha
Gamma + Epsilon
MUC5B+ Ductal
Delta
Beta
Ductal
condition
young
old
z-score
B
Alpha Cells: Top 50 DEGs
C
HALLMARK_INTERFERON_GAMMA_RESPONSE
condition
TNFSF10
IL15
TRIM21
DDX60
STAT1
HERC6
DHX58
BATF2
FAS
CDKN1A
MARCHF1
IL7
RTP4
PSMB8
PSMB9
UBE2L6
SP110
TAP1
PLSCR1
NMI
CASP4
RNF213
SOCS3
SOCS1
APOL6
IFIT3
IFI35
IRF9
GCH1
IRF7
MX1
expression
condition
young
old
D
Interferon Gamma Response Genes
Alpha
Beta
Delta
log2FC (old vs young)
log2 FC Ratio (Beta/Alpha)
E
Fold Enrichment
Enrichment score
KEGG Pathways
Enriched Beta
Enriched Alpha
JAK-STAT signaling pathway
NOD-like receptor signaling pathway
Antigen processing and presentation
Toll-like receptor signaling pathway
Necroptosis
Human immunodeficiency virus 1 infection
Pathways in cancer
Proteasome
Influenza A
Hepatitis C
TNF signaling pathway
−log10(FDR)
F
HALLMARK_GLYCOLYSIS
condition
FUT8
EXT1
GNPDA1
POLR3K
KDELR3
LDHA
IER3
ELF3
VLDLR
PLOD2
GMPPB
FKBP4
GALE
NOL3
AK4
SPAG4
ERO1A
STC2
expression
condition
young
old
G
GOBP_AMINO_ACID_METABOLIC_PROCESS
condition
HMGCLL1
NARS2
KMO
PYCR2
ALDH1A1
PLOD2
CTPS2
DCT
MTAP
BCKDHB
ALDH6A1
MAT1A
ADHFE1
FTCD
expression
condition
young
old
H
HPAP - UPenn
Young
Old
Glucagon (pg/100islets)
No Stimuli
AA
AA + Glc^low
AA + Glc^High
AA + Glc^High + Ibmx
No Stimuli
KCl
I
Young
Old
Glucagon (pg/100islets)
Time (minutes)
Amino acid Mixure, 4 mM
J
0.0097
AA stimulation index (fold from Basal)
Young
Old
K
0.0030
KCL stimulation index (fold from Basal)
Young
Old

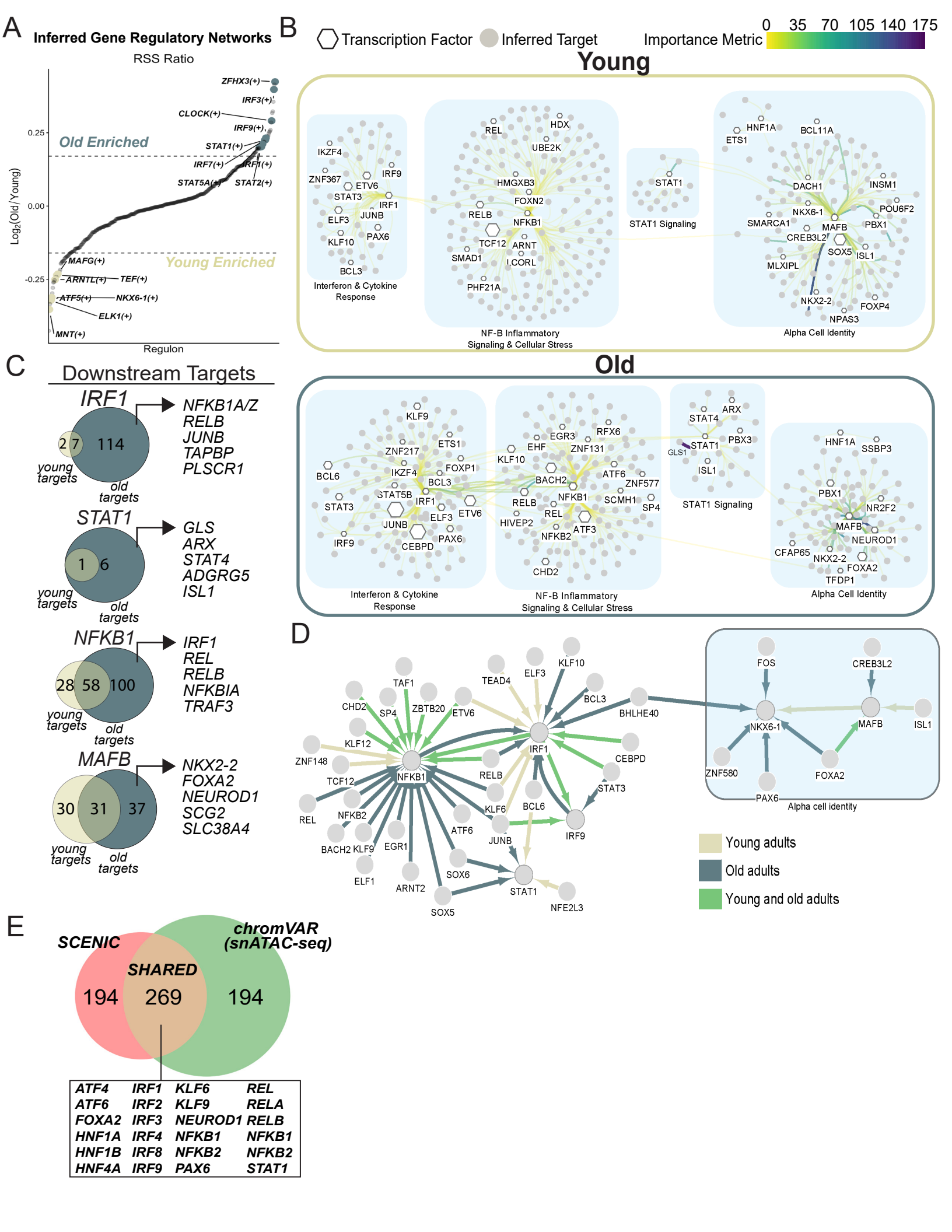
A
Inferred Gene Regulatory Networks
RSS Ratio
Old Enriched
Young Enriched
Log2(Old / Young)
Regulon
ZFHX3(+)
IRF3(+)
CLOCK(+)
IRF9(+)
STAT1(+)
IRF7(+)
IRF1(+)
STAT5A(+)
STAT2(+)
MAFG(+)
ARNTL(+)
TEF(+)
ATF5(+)
NKX6-1(+)
ELK1(+)
MNT(+)
B
Transcription Factor
Inferred Target
Importance Metric
0 35 70 105 140 175
Young
Interferon & Cytokine Response
NF-B Inflammatory Signaling & Cellular Stress
STAT1 Signaling
Alpha Cell Identity
Old
Interferon & Cytokine Response
NF-B Inflammatory Signaling & Cellular Stress
STAT1 Signaling
Alpha Cell Identity
C
Downstream Targets
IRF1
NFKB1A/Z
RELB
JUNB
TAPBP
PLSCR1
2 7 114
young targets
old targets
STAT1
GLS
ARX
STAT4
ADGRG5
ISL1
1 6
young targets
old targets
NFKB1
IRF1
REL
RELB
NFKBIA
TRAF3
28 58 100
young targets
old targets
MAFB
NKX2-2
FOXA2
NEUROD1
SCG2
SLC38A4
30 31 37
young targets
old targets
D
Alpha cell identity
Young adults
Old adults
Young and old adults
E
SCENIC
chromVAR (snATAC-seq)
SHARED
194 269 194
ATF4 IRF1 KLF6 REL
ATF6 IRF2 KLF9 RELA
FOXA2 IRF3 NEUROD1 RELB
HNF1A IRF4 NFKB1 NFKB1
HNF1B IRF8 NFKB2 NFKB2
HNF4A IRF9 PAX6 STAT1

Imaging Mass Cytometry

A

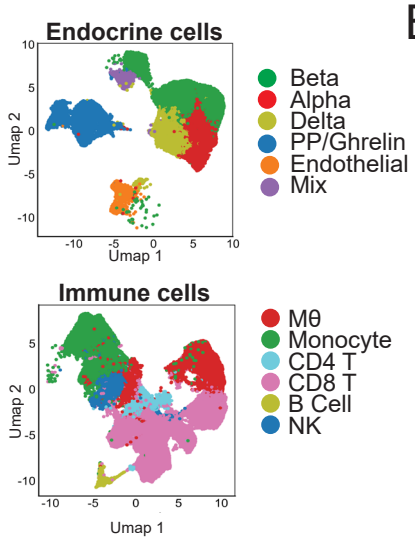

B

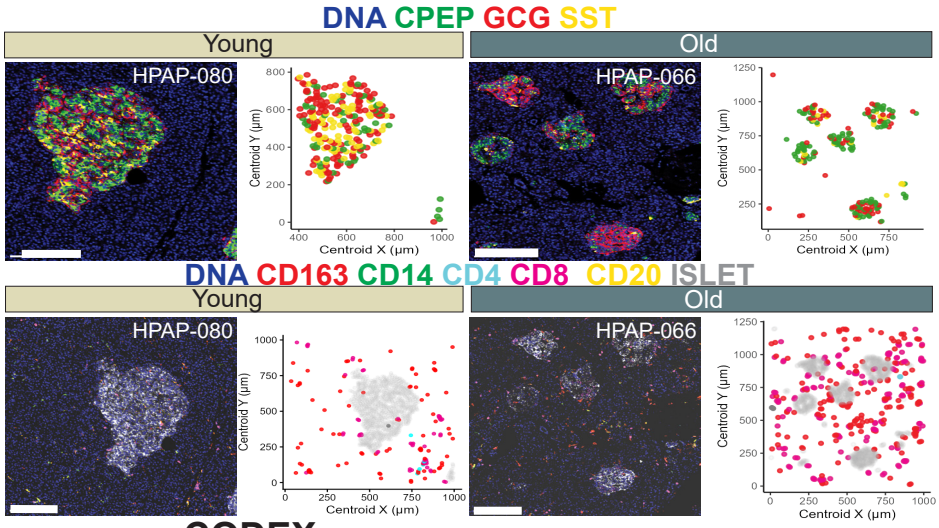

CODEX

C

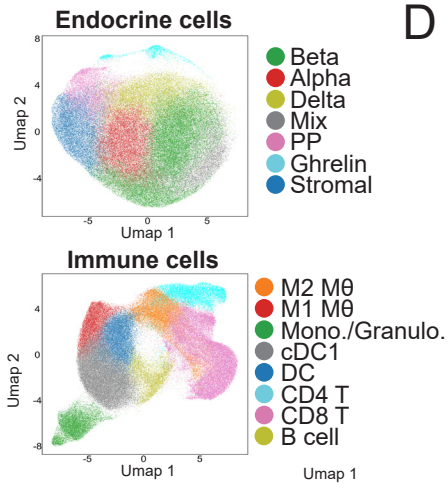

D

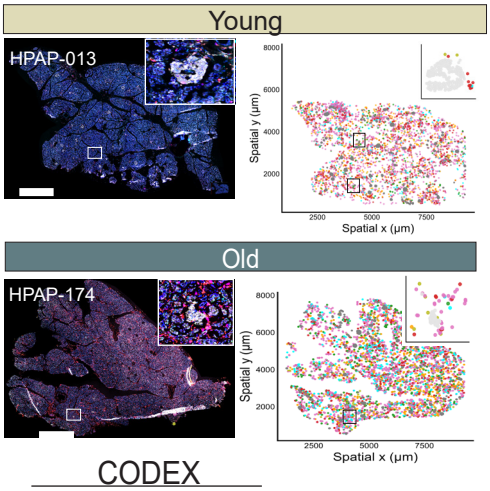

E

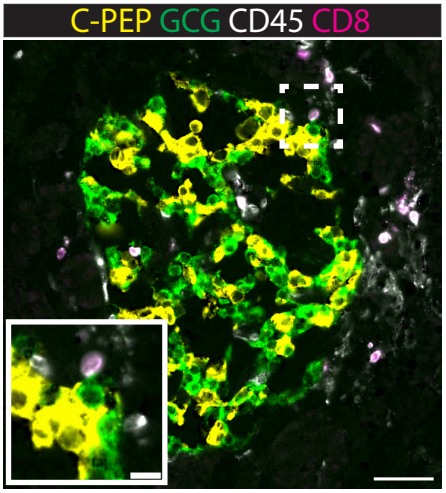

F

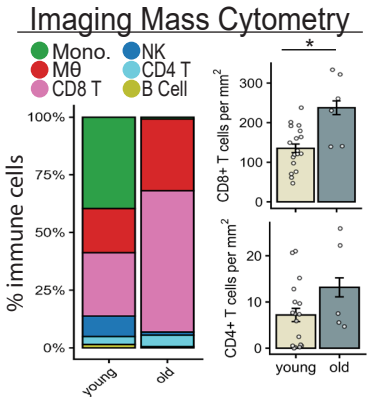

G

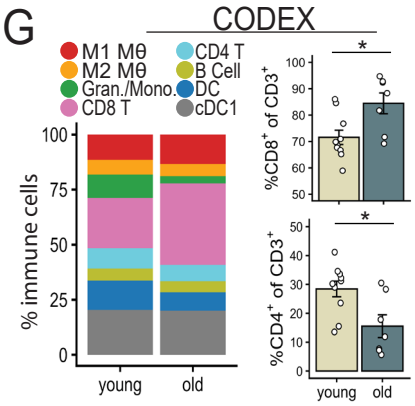

H

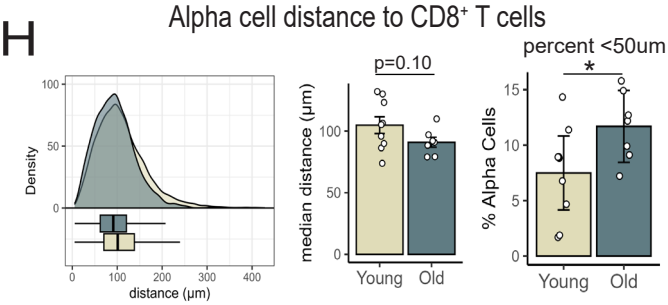

I

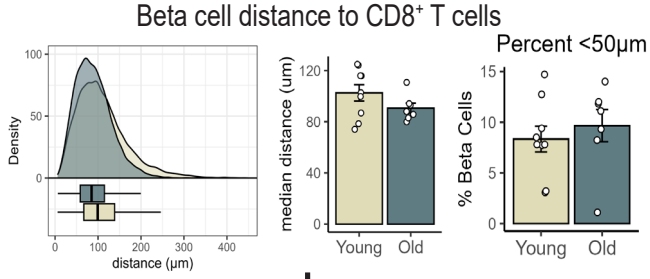

J

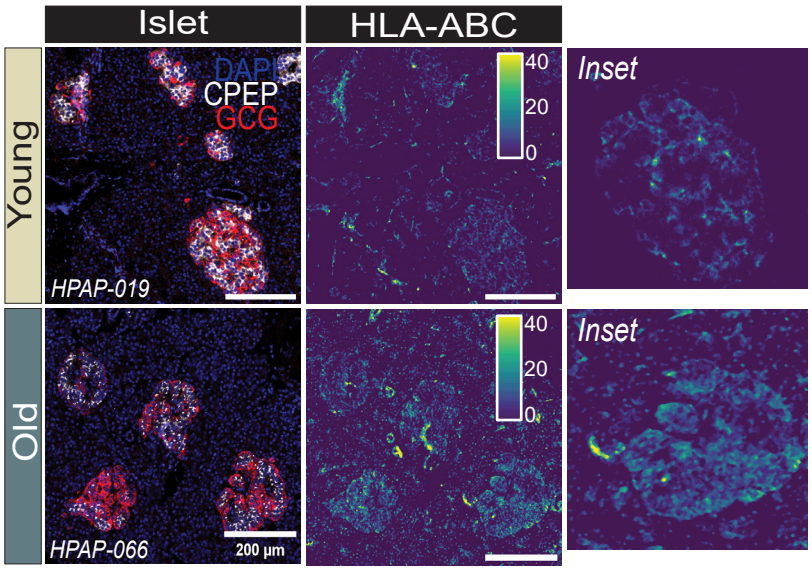

K

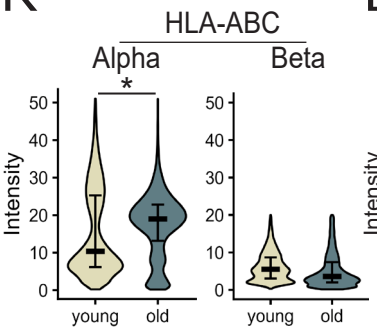

L

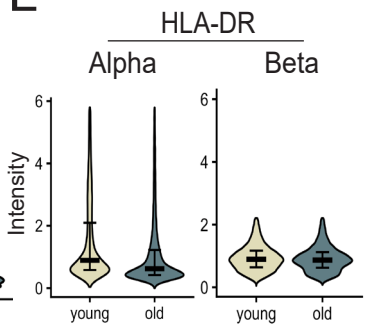

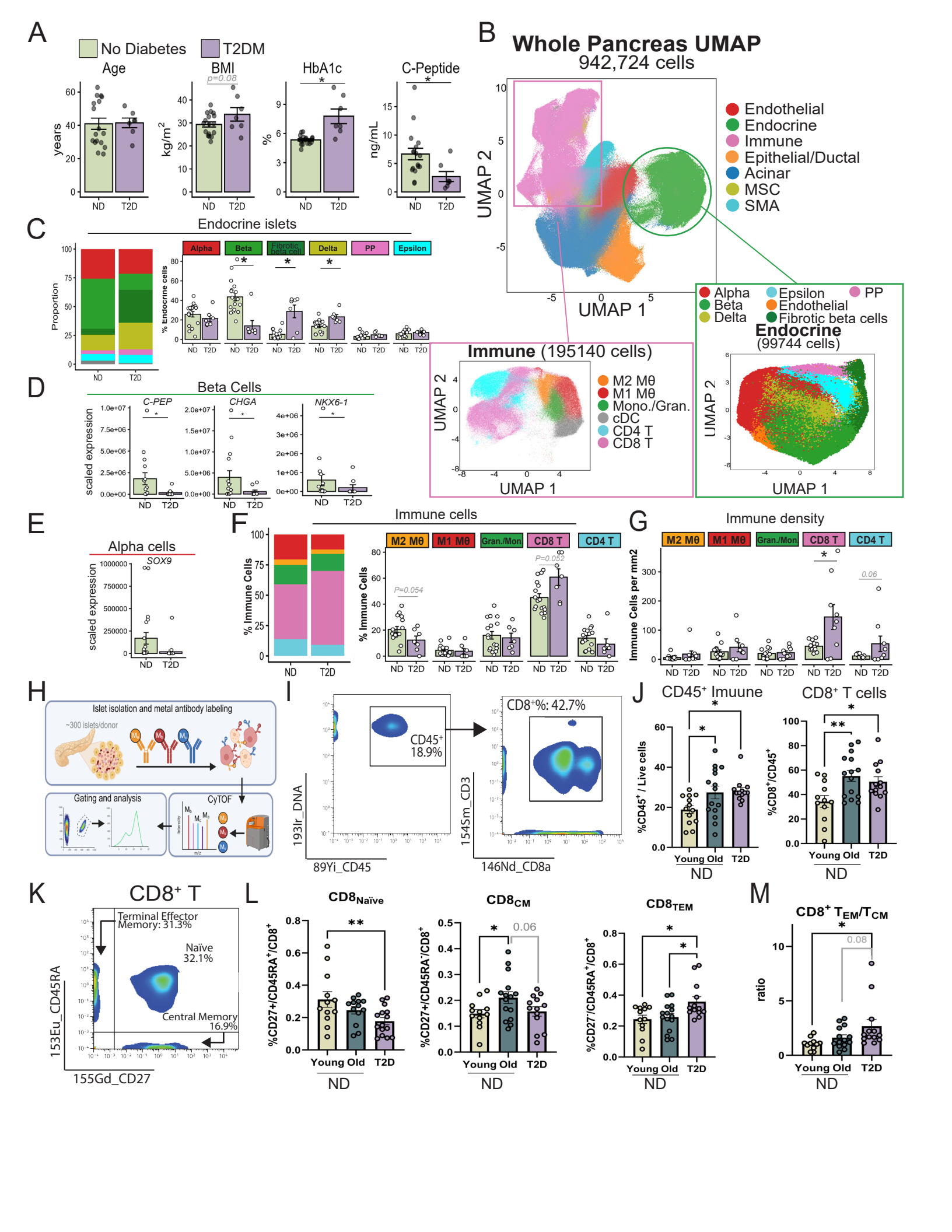
A
No Diabetes
T2DM
Age
BMI
HbA1c
C-Peptide
years
kg/m2
%
ng/mL
p=0.08
ND
T2D
B
Whole Pancreas UMAP
942,724 cells
UMAP 2
UMAP 1
Endothelial
Endocrine
Immune
Epithelial/Ductal
Acinar
MSC
SMA
C
Endocrine islets
Proportion
% Endocrine cells
Alpha
Beta
Fibrotic beta cell
Delta
PP
Epsilon
Immune (195140 cells)
M2 Mθ
M1 Mθ
Mono./Gran.
cDC
CD4 T
CD8 T
Alpha
Beta
Delta
Epsilon
Endothelial
Fibrotic beta cells
PP
Endocrine
(99744 cells)
D
Beta Cells
C-PEP
CHGA
NKX6-1
scaled expression
E
Alpha cells
SOX9
F
Immune cells
% Immune Cells
P=0.054
P=0.052
G
Immune density
Immune Cells per mm2
0.06
H
Islet isolation and metal antibody labeling
~300 islets/donor
Gating and analysis
CyTOF
I
CD45+
18.9%
CD8+%: 42.7%
193Ir_DNA
89Yi_CD45
154Sm_CD3
146Nd_CD8a
J
CD45+ Imuune
CD8+ T cells
%CD45+ / Live cells
%CD8+/CD45+
Young Old
T2D
ND
K
CD8+ T
Terminal Effector
Memory: 31.3%
Naïve
32.1%
Central Memory
16.9%
153Eu_CD45RA
155Gd_CD27
L
CD8Naïve
CD8CM
CD8TEM
%CD27+/CD45RA+/CD8+
%CD27+/CD45RA-/CD8+
%CD27-/CD45RA+/CD8+
0.06
M
CD8+ TEM/TCM
ratio
0.08

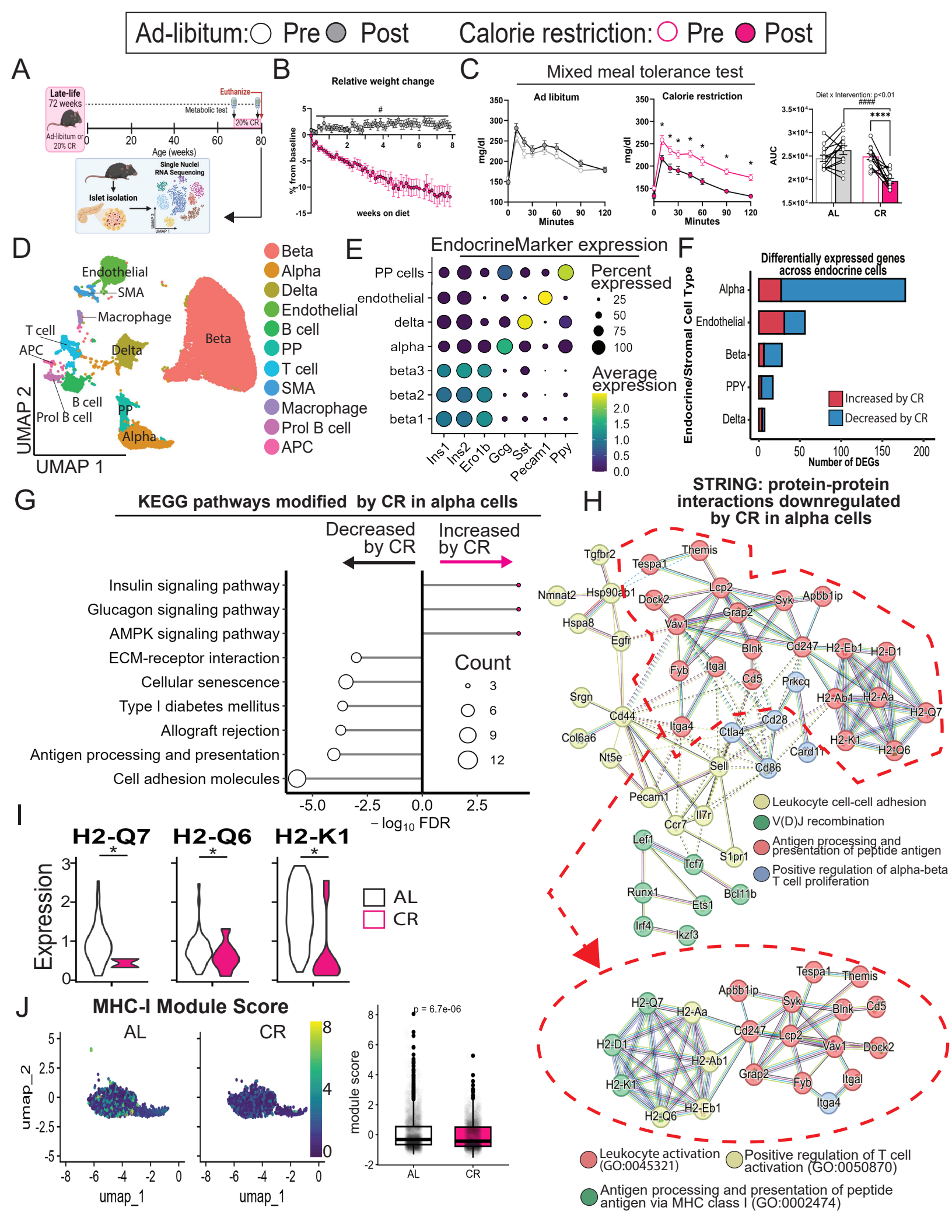
Ad-libitum: Pre Post
Calorie restriction: Pre Post
A
Late-life 72 weeks
Euthanize
Metabolic test
20% CR
Ad-libitum or 20% CR
Age (weeks)
Islet isolation
Single Nuclei RNA Sequencing
B
Relative weight change
% from baseline
weeks on diet
C
Mixed meal tolerance test
Ad libitum
Calorie restriction
mg/dl
Minutes
Diet x Intervention: p<0.01
AUC
AL
CR
D
Endothelial
SMA
Macrophage
T cell
APC
Delta
Beta
B cell
Prol B cell
PP
Alpha
UMAP 2
UMAP 1
Beta
Alpha
Delta
Endothelial
B cell
PP
T cell
SMA
Macrophage
Prol B cell
APC
E
EndocrineMarker expression
PP cells
endothelial
delta
alpha
beta3
beta2
beta1
Ins1
Ins2
Ero1b
Gcg
Sst
Pecam1
Ppy
Percent expressed
25
50
75
100
Average expression
2.0
1.5
1.0
0.5
0.0
F
Differentially expressed genes across endocrine cells
Endocrine/Stromal Cell Type
Alpha
Endothelial
Beta
PPY
Delta
Increased by CR
Decreased by CR
Number of DEGs
G
KEGG pathways modified by CR in alpha cells
Decreased by CR
Increased by CR
Insulin signaling pathway
Glucagon signaling pathway
AMPK signaling pathway
ECM-receptor interaction
Cellular senescence
Type I diabetes mellitus
Allograft rejection
Antigen processing and presentation
Cell adhesion molecules
Count
3
6
9
12
-5.0
-2.5
0.0
2.5
− log10 FDR
H
STRING: protein-protein interactions downregulated by CR in alpha cells
Tgfbr2
Themis
Tespa1
Nmnat2
Hsp90ab1
Dock2
Lcp2
Syk
Apbb1ip
Hspa8
Grap2
Vav1
Egfr
Blnk
Cd247
H2-Eb1
H2-D1
Fyb
Itgal
Cd5
Prkcq
Srgn
H2-Ab1
H2-Aa
H2-Q7
Cd44
Itga4
Cd28
Ctla4
Col6a6
H2-K1
Card11
H2-Q6
Nt5e
Sell
Cd86
Pecam1
Il7r
Ccr7
Lef1
S1pr1
Tcf7
Runx1
Bcl11b
Ets1
Irf4
Ikzf3
Leukocyte cell-cell adhesion
V(D)J recombination
Antigen processing and presentation of peptide antigen
Positive regulation of alpha-beta T cell proliferation
Leukocyte activation (GO:0045321)
Positive regulation of T cell activation (GO:0050870)
Antigen processing and presentation of peptide antigen via MHC class I (GO:0002474)
I
H2-Q7
H2-Q6
H2-K1
Expression
AL
CR
J
MHC-I Module Score
AL
CR
umap_2
umap_1
p = 6.7e-06
module score

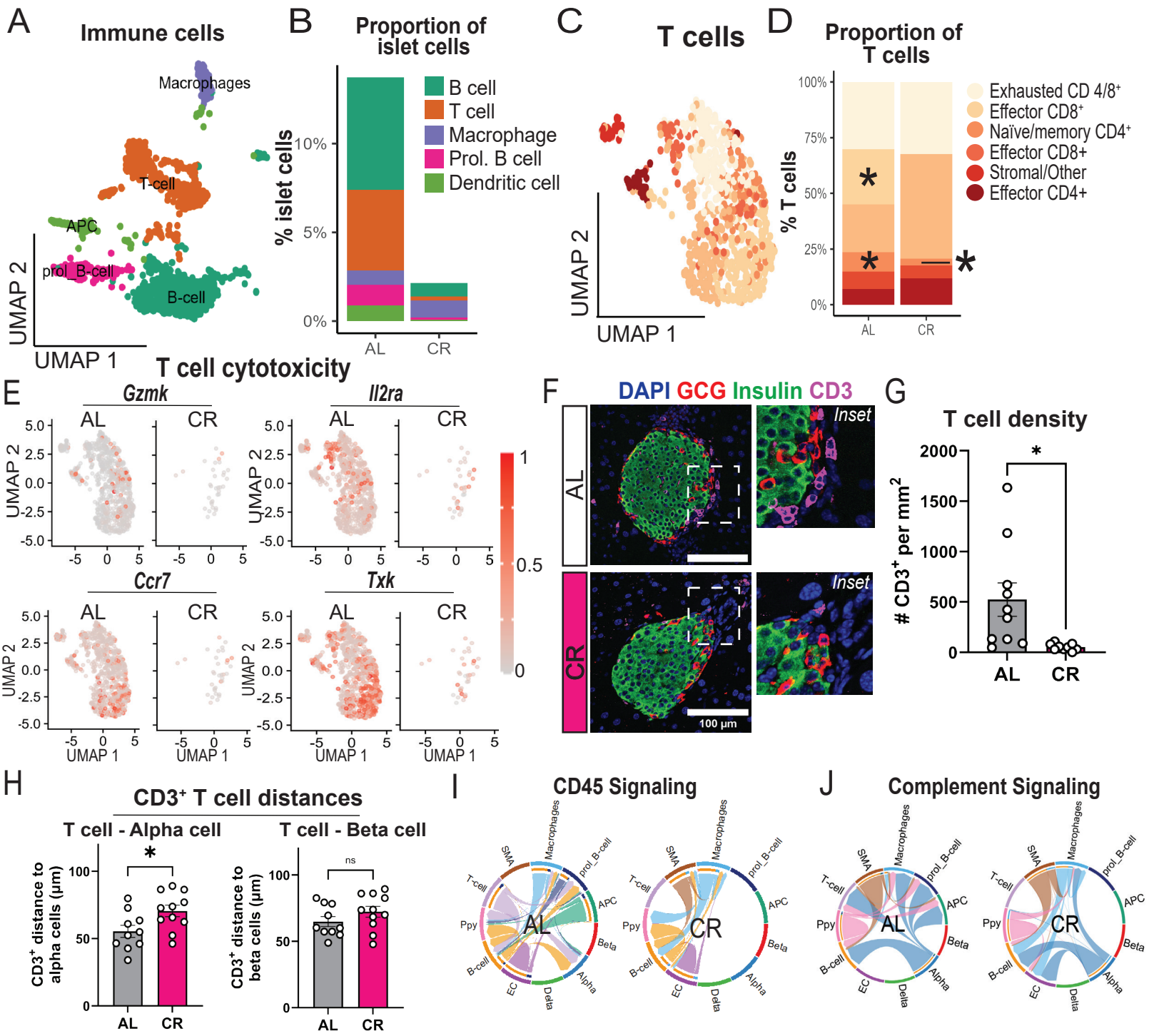
A
Immune cells
Macrophages
T-cell
APC
prol_B-cell
B-cell
UMAP 2
UMAP 1
B
Proportion of islet cells
% islet cells
10%
5%
0%
AL
CR
B cell
T cell
Macrophage
Prol. B cell
Dendritic cell
C
T cells
UMAP 2
UMAP 1
D
Proportion of T cells
% T cells
100%
75%
50%
25%
0%
AL
CR
Exhausted CD 4/8+
Effector CD8+
Naïve/memory CD4+
Effector CD8+
Stromal/Other
Effector CD4+
E
T cell cytotoxicity
Gzmk
Il2ra
Ccr7
Txk
AL
CR
UMAP 2
UMAP 1
1
0.5
0
F
DAPI GCG Insulin CD3
AL
CR
Inset
100 µm
G
T cell density
CD3+ per mm2
2000
1500
1000
500
0
AL
CR
H
CD3+ T cell distances
T cell - Alpha cell
T cell - Beta cell
CD3+ distance to alpha cells (µm)
CD3+ distance to beta cells (µm)
100
50
0
ns
AL
CR
I
CD45 Signaling
Macrophages
prol_B-cell
APC
Beta
Alpha
Delta
EC
B-cell
Ppy
T-cell
SMA
AL
CR
J
Complement Signaling
Macrophages
prol_B-cell
APC
Beta
Alpha
Delta
EC
B-cell
Ppy
T-cell
SMA
AL
CR